A Robotic Head Stabilization Device for Post-Trauma Transport

Adam J. Williams

Thesis submitted to the Faculty of the

Virginia Polytechnic Institute and State University

in partial fulfillment of the requirements for the degree of

Master of Science

in

Mechanical Engineering

Pinhas Ben-Tzvi, Chair

Alfred L. Wicks

Steve C. Southward

May 9, 2018

Blacksburg, Virginia

Keywords: Rescue Robot, Robotic Systems, Mechatronics, Head Stabilization

A Robotic Head Stabilization Device for Post-Trauma Transport

Adam J. Williams

ABSTRACT

The work presented in this thesis focuses on the design and testing of a casualty extraction robot intended to stabilize the head and neck of an unresponsive person. The employment of robots in dangerous locales such as combat zones or the site of a natural disaster has the potential to help keep first responders out of harm's way as well as to improve the efficiency of search and rescue teams.

After a review of robotic search and rescue platforms the Semi-Autonomous Victim Extraction Robot(SAVER) is introduced. The necessity of a device intended to support the head and cervical spine during transport on a rescue robot is then discussed. The kinematic and dynamic analyses of various candidate differential mechanisms intended for the head stabilization device are described, and the chosen mechanism is demonstrated in a proof-of-concept device. Following testing with a simple PID controller, it was determined an advanced feedback controller with disturbance rejection capabilities was required. Linear Active Disturbance Rejection Control (LADRC) was chosen for its effectiveness in rejecting perturbations and handling modeling uncertainties. The performance the proposed LADRC control scheme was compared with PID in simulation and the results are presented. Finally, a prototype of the device was designed and built to validate the functionality of the subsystem, and the results of the corresponding experimentation are discussed.

A Robotic Head Stabilization Device for Post-Trauma Transport

Adam J. Williams

GENERAL AUDIENCE ABSTRACT

Robots can help to keep first responders and medics out of dangerous situations by performing the rescue operation themselves or by collaborating with the field medic to make the process quicker and more efficient. The work presented in this thesis begins with a review of state-of-the-art rescue robots followed by the a brief description of the design of a Semi-Autonomous Victim Extraction Robot (SAVER) intended to rescue injured and incapacitated people. After the SAVER system is briefly described, the necessity of a device intended to support the head and cervical spine during transport is discussed. The head stabilization subsystem could also be implemented as a standalone device for use by paramedics to help free up valuable time that would otherwise be spent in manually stabilizing the head and neck of the injured person.

Acknowledgments

I would like to extend my gratitude to the many people who made my graduate research possible. Firstly I would like to thank my advisor, Dr. Pinhas Ben-Tzvi, for his tireless guidance, support, and motivation. Additionally, I would like to thank the US Army Medical Research & Materiel Command's Telemedicine & Advanced Technology Research Center (TATRC). This work is supported in part by the US Army Medical Research & Materiel Command's Telemedicine & Advanced Technology Research Center (TATRC), under Contract No. W81XWH-16-C-0062. The views, opinions, and/or findings contained in this report are those of the authors and should not be construed as an official Department of the Army position, policy, or decision unless so designated by other documentation.

I would also like to thank my colleagues from the Robotics and Mechatronics Lab: Peter Racioppo, Anil Kumar, Hailin Ren, Vinay Kamidi, Brielle Lee, Will Rone, Wael Saab, Eric Refour, Taylor Njaka, Ravi Chauhan, and Dan Budolak for their help and friendship over the duration of my graduate career. I owe special thanks to Bijo Sebastian for lending his expansive knowledge and patience in assisting and mentoring me throughout my time in

RML.

I want to extend my thanks and send my love to my parents and my brothers for all their support over the years. Finally, I would like to thank my wife Perisa for her love, guidance, and understanding throughout this entire process.

Contents

List of Figures

List of Tables

Chapter 1

Introduction

1.1 Background

The utilization of robots can greatly increase the speed and efficacy of search and rescue operations, especially in the aftermath of natural disasters or combat scenarios. While robots are becoming more and more common in the search aspect of search and rescue operation, there have been very few platforms intended to be implemented in a search capacity. The enabling technology for such systems is still in its early stages, due to limitations in actuators, controls, and safe human-robot interaction.

Locating and transporting a wounded person with a robot is a complex task of great relevance due to the hostile environment that prevails after a disaster or during combat. Sending in human rescue personnel into this hostile environment could endanger the search teams. In

addition to improving victim outcomes, rescue robots also have the potential to improve the efficiency and effectiveness of search teams when working alongside them. First, robots can enter environments before humans can when noxious gasses, radiation, or other hazards are present. In addition, if a rescue robot can work in collaboration with the first responders to transport incapacitated individuals from a dangerous locale to safety, the number of humans required per rescue team could be reduced and facilitate a wider dispersion of trained medical and rescue personnel throughout a disaster zone. Furthermore, with proper design, robots can run continuously with just a momentary stop to switch out battery packs or refuel, facilitating nonstop search efforts while human team members can divide shifts more effectively and receive more rest time. The thesis presented here describes the initial design of such a rescue robot, and goes into further detail on the design and testing of a particular subsystem of said rescue robot intended to stabilize the head and cervical spine of the person being transported.

Per the U.S. Department of Transportation National Highway Traffic Safety Administration, when a first responder encounters a person who may have suffered a traumatic injury, the accepted standard operating procedure is to bring the cervical spine into the neutral position, then fit a stabilization unit to the patient [25]. The goal is to minimize translation and rotation of the head in order to avoid aggravating spinal injuries during lifting or transport. Classically, the prescribed methods for post-trauma stabilization include a two-fold strategy of fitting a cervical collar to the patient's neck, followed by immobilizing the head of the patient utilizing some form of head supporting framework. However, recent work illustrating

the contributions of cervical immobilization to patient mortality and morbidity have led to a concerted effort to explore the reduced use of a cervical collar in trauma situations [26]. These findings led to the omission of a cervical collar component in the presented design, due to the complexity and expert-level training required for the safe placement of such devices.

The described scenario thus forms the basis for the system presented herein, a robotic head stabilization system that autonomously stabilizes the head and neck of a patient, allowing them to be transported on autonomous rescue robots or freeing up first responders to perform other potentially life saving actions.

1.2 Statement of Contributions

This thesis presents a novel robotic head stabilization device that utilizes a differential mechanism and linear active disturbance rejection control to provide support to the head of an unresponsive person. In addition, the Semi-Autonomous Victim Extraction Robot, of which the head stabilization device is a subsystem, is described in detail and its operation is presented. In addition to conceptual designs, both a proof-of-concept model as well as a final prototype of the head stabilization device were developed. In the field of rescue robotics, the work of this thesis presents the following contributions:

1. A novel head stabilization device capable of providing stabilizing support to the head of a transported patient in order to help prevent against further aggravation of injury, actions that have not yet been performed by an robotic system.

2. Implementation of a series elastic actuator in order to indirectly measure the force applied by a mechanical system through application of a derived model.

3. Adaptation of linear active disturbance control, an observer based feedback control method, for use with a force-controlled mechatronic system.

1.3 Thesis Struture

This thesis is organized as follows:

Chapter 1: Presents the introduction and contributions of this thesis

Chapter 2: Provides a comprehensive literature review of the current state of the field of search and rescue robots that have been implemented in the field

Chapter 3: Describes the design of the robotic head stabilization system

1.4 Selected Publications

Disclosure: *Content from these publications was used throughout this thesis.*

Conference Papers:

1. **Williams, A.**, Saab, W., Ben-Tzvi, P., "Analysis of Differential Mechanisms for a Robotic Head Stabilization System", Proceedings of the 2017 ASME IDETC/CIE,

41st Mechanisms & Robotics Conference, Cleveland, Ohio, Aug. 6-9, 2017.

2. Sebastian, B., **Williams, A.**, Ben-Tzvi, P., "Control of a Head Stabilization System for Use in Robotic Disaster Response", Proceedings of the 2017 ASME International Mechanical Engineering Congress and Exposition (IMECE 2017), Tampa, Florida, Nov. 3–9, 2017.

Journal Papers:

1. **Williams, A.**, Sebastian, B., Ben-Tzvi, P., "Review and Analysis of Search, Extraction, Evacuation, and Medical Field Treatment Robots", *Journal of Intelligent & Robotic Systems*. Submitted, October 2017.

2. **Williams, A.**, Sebastian, B.,Ben-Tzvi, P., "A Robotic Head Stabilization Mechanism for Medical Transport", Journal of Mechanisms and Robotics, Submitted, March, 2018.

Chapter 2

Literature Review

2.1 Robotic Impact on Search and Rescue Operations

Many deaths ocurring in the aftermath of natural disasters as well as combat are due to treatable traumatic injuries, and could be avoided if it were possible to provide medical treatment in a timely manner [27, 28]. This notion of time-sensitive treatment is represented by "The Golden Hour of Trauma" [29, 30, 31, 32], the theory that if medical assistance is provided within a short time following traumatic injuries, the survival rate of the injured person rises appreciably. While the debate on the exact definition and duration of this critical period is unresolved in the medical literature, a mandate from the Secretary of Defense in 2009 to prioritize transporting military causalities in an hour or less resulted in a significant decline in mortality due to traumatic injuries, especially those requiring blood

transfusions [33]. As hemorrhage due to major trauma has been found to be the cause of death in up to 80% of potentially survivable wounds in the U.S. military, timely evacuation and transportation must be an emphasis when working to improve medical care [34]. This emphasis has led to the U.S. Army Medical Research and Material Command reopening investigation in this field [35].

While rapid medical assistance constitutes a major key in reducing traumatic fatalities, the need for rapid response must be balanced against the risks to the safety of the men and women providing the assistance in rescue situations [36]. Deploying a rescue team into a combat scenario or the aftermath of a natural disaster may not only endager the lives of the rescuers but also of those being rescued. In addition, in acts of terrorism or active combat, a commonly seen strategy is the use of "leave behind" ordinance in order to injure or kill the first responders attemping to assist the victims of the inital attack [27]. Moreover, catastrophic events often occur in remote locations, making it difficult to reach the area where help is required or to maintain communication between teams. For each of the mentioned cases, robots can assist and augment first responders and medical teams to make their work more efficient and keep them safe.

The current state of the search and rescue robotics field can be segmented into four groups representative of where a system participates in a search and rescue mission: search, extraction, evacuation, and treatment [10]. In the search stage,robots work to find and relay back to a central command center the location of any injured persons. The use of robots in this manner is a mature operation, and has been conducted in the field as early as the aftermath

of the September 11th attacks [37]. Following the location of an injured person is the extraction stage, in which a robotic system physically maneuvers or transports the injured person to a location of safety. While a less mature area of research than that of search, these 'rescue' robots are by necessity larger and at times more complex systems than their search-focused brethren. Systems such as the Battlefield Extraction-Assist Robot (BEAR) and the Robotic Extraction Vehicle (REX) are indicative of these types of robots [38, 39]. Following the safe extraction of an injured person from a dangerous area, there must be safe and efficient evacuation of the patient to an area where medical assistance can be administered. The robots that are designed to perform this task come in a variety of forms, including the LSTAT, a stretcher with a full set of sensory equipment and a robotic snake-like manipulator, [40], and the Robotic Evacuation Vehicle (REV), a mobile patient transport robot [38]. Once at a more advanced medical station, in this envisioning of a futuristic roboticized rescue mission robotic surgical systems are utilized in the treatment of the wounded person by allowing a remotely located surgeon to perform advanced surgical procedures in situ. While early robotic surgical systems such as the da Vinci [20] and the Zeus [41] were designed for this purpose, they are too large to be utilized to conduct operations in the field. In order to improve designs for remote in situ usage, the next generation of surgical robots emphasize compact footprints and improved communication latency compensation.

The future of medical and rescue robotics is to fuse the varied components of a search and rescue team into a cohesive collaborative robotic unit that can be interwoven into the search and rescue process from start to finish. In this scenario, following the arrival of first

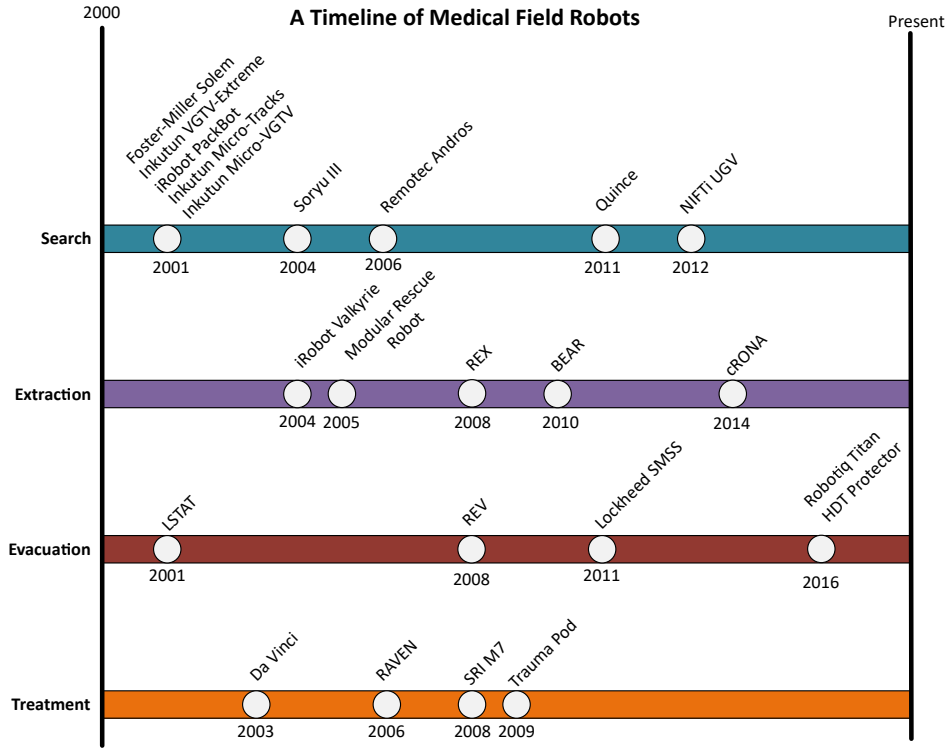

Figure 2.1: A timeline of the search, extraction, evacuation, and treatment robots reviewed in this work

responders in the aftermath of a calamity, the robotic systems are immediately deployed in tandem with first responders. The robots collaborate with each other and with the first responders to locate any injured personnel within the disaster scene, extract them from the danger zone, then safely evacuate them to a field hospital. At the forward medical center, top surgeons from around the world are able to offer their expertise remotely through robotic surgery systems.

2.2 Search Robots

Robots can have great ability to explore affected regions and locate people in distress during the aftermath of disasters or combat. These robots are generally designed to act as mobile sensory platforms and perform small yet crucial tasks. This enables the use of sophisticated detection sensors in scenarios that may be unsafe or unreachable for human rescuers [42]. Furthermore, with proper design, robots can run continuously, with only a momentary stop for refueling. Serve interchangeability facilitates nonstop search efforts and allows human team members to divide shifts more effectively and receive more rest time. A major detriment to search and rescue efforts, particularly when operating high-level technology, is the impairment of cognitive functions caused by sleep deprivation [6]. The search robots graphi-

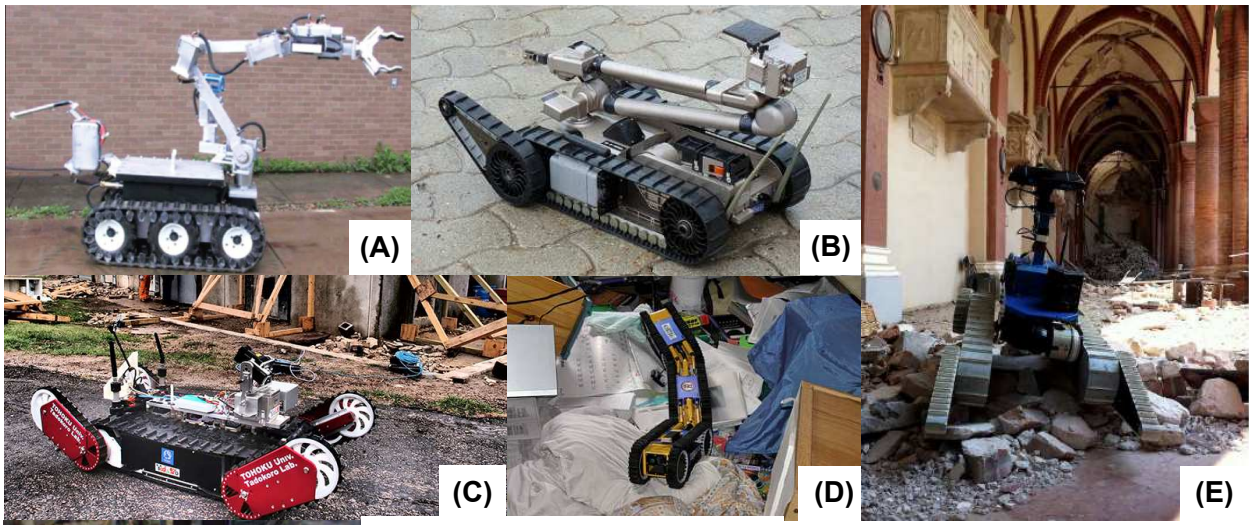

Figure 2.2: (A) Remotec Wolverine [1] (B) iRobot PackBot [2] (C) Quince [3] (D) Soryu III [4] (E) NIFTi UGV [5] (F) Foster-Miller Solem [6] (G) Inkutun VGTV-Xtreme (Inkutun, 2017) (H) Inkutun Micro-VGTV and Micro-Tracks [6] [7]

cally compared herein are shown in Fig. 2.2. Further discussion of their specific capabilities are contained in [7].

Spurred by the close succession of the catastrophic 1995 Oklahoma City bombing and Kobe earthquake (Davids, 2002), research into outfitting unmanned aerial vehicles (UAVs), unmanned ground vehicles (UGVs), and autonomous underwater vehicles (AUVs) with search capabilities was initiated. Robot-human teams were deployed to probe the rubble of the World Trade Center following the attacks on September 11th in 2001, UAVs were used to assist in the search for those trapped by the flooding resulting from Hurricane Katrina in 2005, an AUV surveyed the damage to the Rollover Pass Bridge caused by Hurricane Ike in 2008, while in Japan mobile robots such as Quince were utilized to measure the radiation in the aftermath of the Fukushima nuclear disaster in 2011 [43, 4, 44, 45].

Based on the past deployments of robots in disaster scenarios, contributions to search efforts can be divided into three broad categories: conducting a survey of the scenario to estimate the extent of damage and the stability of structures, collecting data for exploration to be used by rescue teams (such as 3D maps of the interiors of buildings), and looking for potentially injured persons. In order to perform the above functions effectively, the robots are generally designed to be small (man-packable), agile, and requiring only a small degree of supervision from the human operator. Most of the commonly used UGV systems were initially developed for military purposes such as Explosive Ordnance Disposal (EOD). However, these robots have been modified for search and rescue to be much smaller than their corresponding military systems, so that they can fit into openings that people and dogs cannot enter.

In addition to the mature and field tested systems pictured here, there are many innovative robotic systems built for search and rescue applications that have yet to see field use. Wolf et al. designed a mobile hyper-redundant robot consisting of a snake-like manipulator mounted on a mobile base [46]. The flexible manipulator was designed to enable the robot to better investigate small features such as cracks as well as manipulate its search camera to more effectively explore its environment [47]. Another unique design for a search and rescue robot is the Hybrid Mechanism Mobile Robot (HMMR), which consists of three links(two tracked and one central), one housing the manipulator and possessing the ability to rotate 360 degrees [48, 49]. By leveraging the robot's operational symmetry, i.e. its ability to operate in multiple orientations, and its multitude of locomotion modes, the HMMR is uniquely suited to navigating the unstructured terrain encountered in the aftermath of a disaster [50]. Another wide-ranging effort to build effective search and rescue robots is the ICARUS project, an EU-backed proposal made up of a collaboration of universities and private companies, which has a wide array of autonomous and semi-autonomous systems intended for search and rescue, including solar powered search UAVs, heavy UGVs with a crane arm, and smaller UGVs for searching buildings [51, 52]. Components have been field tested and demoed, but have yet to perform in an actual disaster situation.

When it comes to searching a disaster environment, robots can now provide a remote presence for rescuers in areas that are physically inaccessible or unsafe, while also allowing the rescuers to "sense and act at a distance" [53]. In comparison to existing active or semi-active articulated cameras used for similar tasks, robots can go further into the rubble while also

interacting with the environment in manners such as taking samples or closing valves via a manipulator. Additional capabilities, such as the ability to work indefinitely without tiring and possession of a wide array of sensors used for tasks such as detecting toxic or explosive gasses in the environment, make robots better equipped for search activities when compared to a human or animal counterpart. Above all, robots should be used in scenarios where there is a risk to the life of the rescuers. Thus, key factors in the advantage of robots over other search systems are their terrain adaptability and ability to interact with the environment. With the advancement of research, we can have robot-human teams that allow for faster coverage of the disaster environment, allowing for better allocation of resources and a collaborative system that performs better than the sum of its parts. Figure 2.3 below graphically depicts a comparison between the review systems ability to interact with the environment and adapt to the local terrain.

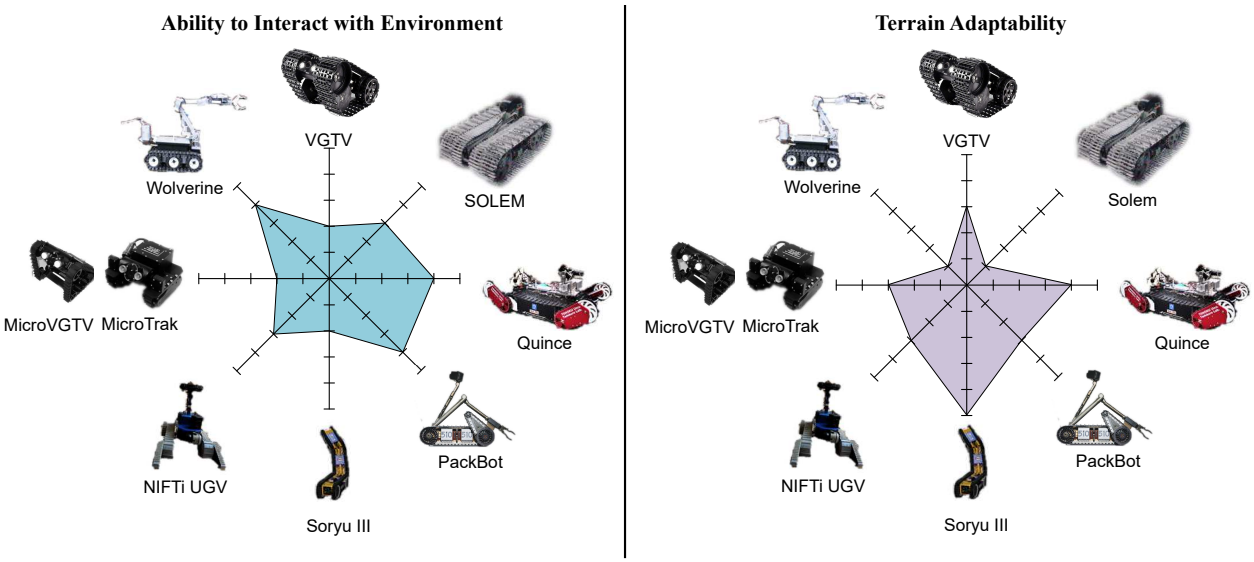

Figure 2.3: Graphical comparison of key search robot abilities [7]

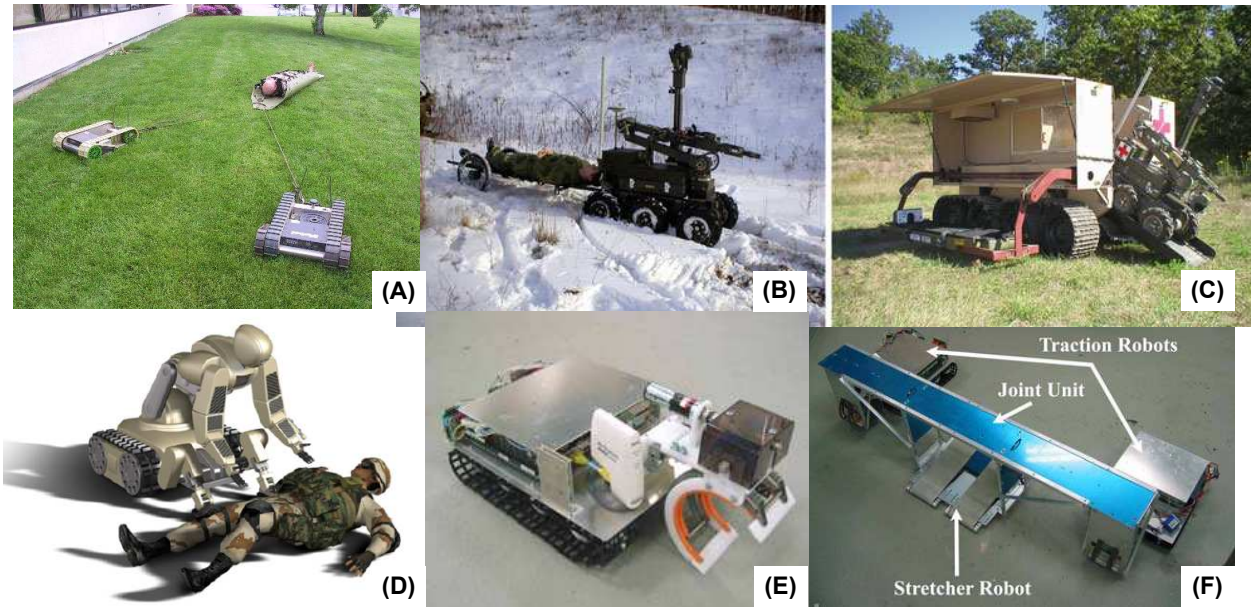

Figure 2.4:) iRobot Valkyrie [8] (B) REX [9] (C) BEAR [10] (D) cRONA [11] (E) Modular Rescue Robot (Traction Robot) [12] (F) Modular Recue Robot [13]

2.3 Extraction Robots

Extraction of a wounded person using a robot is a complex task due to the necessary interaction between a robot and an injured, and possibly incapacitated, person. However, human-robot interaction is a rapidly expanding field and improved actuators and controllers are in active development to enhance these interactions. Due to the technological limitations that still exist, this area is less advanced than that of search robotics, but is quickly growing in recent years. The extraction robots reviewed in this work are pictured in Fig. 2.4.

iRobot Valkyrie: One of the earliest solutions to the robotic casualty extraction problem was created by iRobot in 2004, called Valkyrie [54]. Funded by the Army Telemedicine and

Advanced Technology Research Center (TATRC), it had evolved from iRobot's earlier medic robot, Bloodhound [40]. Valkyrie was a modification of the company's man-packable UGV Packbot, consisting of a deployable flexible stretcher called a Sked tethered to the robot. In theory, a medic could remotely operate the Valkyrie from a position of safety, sending it out to rescue an injured soldier in a dangerous situation. Once the robot reached the injured solider, either nearby squad members or the soldier would secure themselves in the Sked, and the robot would drag the Sked to safety.

With no active manipulators or extra degrees of freedom, a single joystick mounted on an Operator Control Unit would be sufficient to operate the robot, provided the OCU possessed a video feed or the operator had line-of-sight contact with the robot. The operator would just need to drive up to the target, turn around the robot, and then deploy the stretcher. Once the injured person was on board, the robot would simply need to be driven back to safety. The feasibility of this design hinges on either the injured person or someone at hand being capable of securing the injured party within the Sked. Unfortunately, relying on third party intervention decreases the efficacy of the system, while expecting the injured person to secure himself within the Sked was not always feasible. Moreover, in cases where a single PackBot is incapable of dragging the Sked, as seen in Fig. 2.4(A), multi-robot control becomes a concern. Using multiple mobile robots to drag a single object through non-uniform terrain with obstacles and rough patches while maintaining formation is still an active research problem. A positive factor is that by incorporating an existing platform into the design, operation, repairs, and maintenance would be standardized with a system

that has already been field-tested. In all, the Valkyrie was an excellent modification of an existing platform. Unfortunately, this simplicity was also a drawback as the approach itself would be feasible only within limited scenarios.

Robotic Extraction Vehicle (REX): The Robotic Extraction and Evacuation system was a "marsupial" robotic system in that the larger and faster Robotic Evacuation Vehicle (REV) transports a smaller Robotic Extraction Vehicle (REX) that was deployed near the extraction site [10, 40, 9]. The system was designed by Applied Perceptions Inc. in collaboration with TATRC. Like the Valkyrie, the extraction robot REX was intended to reach a wounded soldier and place them onto a stretcher, which was pulled behind the robot. In this case, rather than dragging the stretcher on the ground, the REX would tow a wheeled stretcher. After performing the rescue and returning to the REV, the wounded would be loaded into stretcher bays on the evacuation vehicle, and then the faster REV would provide transport to the nearest medical station.

REX was designed to utilize its single manipulator to pull a wounded solider onto its stretcher. If the soldier was unconscious, he or she must be maneuvered onboard with the single pincer, which may be challenging if the stretcher is not on perfectly flat terrain. Significant operational control is required to grasp an unconscious person using a single pincer end effector without causing new injuries or aggravating existing ones. Unless the wounded soldier was capable of getting on the stretcher on his/her own, this extraction strategy was time consuming and rather inefficient. The use of a rolling stretcher allowed for ease of transport, but presented additional difficulties when trying to load a wounded solider onboard.

In addition, the two-wheeled stretcher could present a tipping and maneuvering hazard in rough terrain and limited space scenarios. Since both the REX and Valkyrie systems were EOD platforms redesigned for casualty extraction, their ability to manipulate and transport injured personnel safely and securely was limited.

BEAR: One of the most developed casualty extraction robots to date is the Battlefield Extraction Assist Robot (BEAR), built by Vecna Robotics [55]. BEAR was a semi-anthropomorphic tracked robot designed with an emphasis on agility and maneuverability. The name is both an acronym and a reference to the head segment that houses its primary sensing array, designed to resemble a teddy bear in order to make the robot less threatening when interacting with humans [56]. BEAR incorporated dynamic balancing behavior in order to enhance its already agile design, allowing it to extend its tracks to be perpendicular to the ground and "stand" or to move in a more traditional manner with its tracks flat on the ground [57, 55]. The torso had several degrees of freedom, allowing the robot to navigate tight spaces while carrying a heavy load by utilizing hydraulic actuation. The most recent prototype found in the literature had 22 degrees of freedom [39]. BEAR had two arms, ending with either mitten-like or simple clawed end effectors in order to facilitate the act of sliding them under the wounded.

BEAR's high DOF design required very advanced controls, and its multiple modes of travel added another layer of complexity. As described in the patent filed for BEAR, possible control methods include a multi-joystick operator control unit or a motion capture suit intended to couple the movements of the robot with the real time movements of the wearer

[55]. While a motion capture suit would help make the operation more straightforward, it would still struggle to provide entirely intuitive control and could suffer from communication delays during remote operation. The transport method utilized in the design of BEAR was optimized for picking up a person rather than conveying them as safely as possible. As shown in the Fig. 2.4(C), the primary extraction method of the robot was to carry the wounded in its arms, which was the simplest configuration that can be achieved with a two-armed robot. There is less risk of further injuring a person when using two arms that go underneath the body rather than using a single manipulator. However, this design assumed the injured person has no head or neck trauma that require the head/neck to be supported or immobilized in transport, as BEAR simply let it fall limp with no restraint. So while the robot is able to get a person into its arms in the most effective manner available to it, there was much to be desired in terms of the health and safety of the injured during transport.

cRONA: Similar to BEAR, cRONA was a humanoid robot that used two arms to lift up an injured person and carry them to safety while utilizing tracks as its primary form of locomotion [58]. Based on a previously designed Robotic Nurse Assistant (RONA), the cRONA was the combat variant. RONA utilized a holonomic drive to provide greater mobility, positioning itself in front of a hospital bed then bending and sliding its two arms under the patient in order to help transfer them from bed to gurney and back [59]. Capable of lifting up to 300 lbs. and utilizing specially designed series elastic actuators to implement force control, RONA was intended to utilize compliant manipulators to lift humans while minimizing the possibility of causing further injury [60]. cRONA operates in a similar way, approaching an

injured soldier, then bending down to gently lift them and either carry them to safety in its arms or load the wounded onto a stretcher pod, which was then towed by the robot [61]. The pods have the ability to be linked together to form a train, allowing cRONA to rescue multiple wounded persons.

While the lifting methodology of the robot faced the same challenges as that of BEAR, these problems were somewhat mitigated when cRONA was operating in tandem with the proposed stretcher pod, as the pod provided a secure and supportive transport vehicle for the wounded. This enclosed stretcher was described in the patent as possibly being motorized and providing some automated medical services, however work on such a pod beyond the patent description has not been described in the literature. In addition, such a stretcher pod presented a high risk of tipping in addition to possibly struggling to traverse rough terrain. The robot also possessed stabilizing legs such as those found on heavy mobile cranes, in order to allow the robot to have a much reduced track area and still not tip when lifting a person. These smaller tracks should be able to guarantee drivability when operating in most terrain conditions, but may also result in greater difficulty balancing on rough or non-level terrain with a robot as tall as cRONA.

Modular Rescue Robot System: Another notable solution to the extraction problem is the modular patient transport system designed by Iwano et al., intended to help the injured persons in the wake of a nuclear power plant meltdown [62]. The team of small robots was designed to approach a prone person and readjust them into an acceptable posture for transport [13]. Robots equipped with cuff-like grippers would grab the supine person's limbs

and manipulate them into a better pose. Then, a rolling platform would slide under the body to act as a stretcher base. The remaining robots would then provide the actuation and guidance for the person on the rolling stretcher [12]. This system was well designed, but meant to operate only on the smooth concrete surfaces and large areas of a nuclear power plant. Attempting to utilize this system in a rough environment would face major challenges, especially when coordinating the robots in a confined space or carrying someone over uneven ground. In its most recent incarnation, the system is shown as a rescue support stretcher intended to allow a single rescuer maneuver an incapacitated person through underground areas and stairs, and the modular reconfigurability of the system is no longer a centerpiece of the design [63]

The designs for extraction robots reviewed here attempt to balance complexity of operation with specificity of function. Systems such as Valkyrie and the REX are much simpler to control than the others, but lack the ability to effectively transfer the injured person onboard. On the other end of the spectrum, cRONA and BEAR are fully articulated humanoids capable of gently picking a person up in their arms. However, this complexity comes at a high control cost, with a multitude of actuators and sensors requiring high bandwidth communications, complex controller design, and high level computing. Both categories of systems have merits, yet further work can be done to find a more effective combination of the two. However, it can be seen that the major differentiating factors in terms of functionality between these systems are the stability of the injured person during the transfer from the robot to the ground and the stability during transit to the medical site. In Fig. 2.5, the

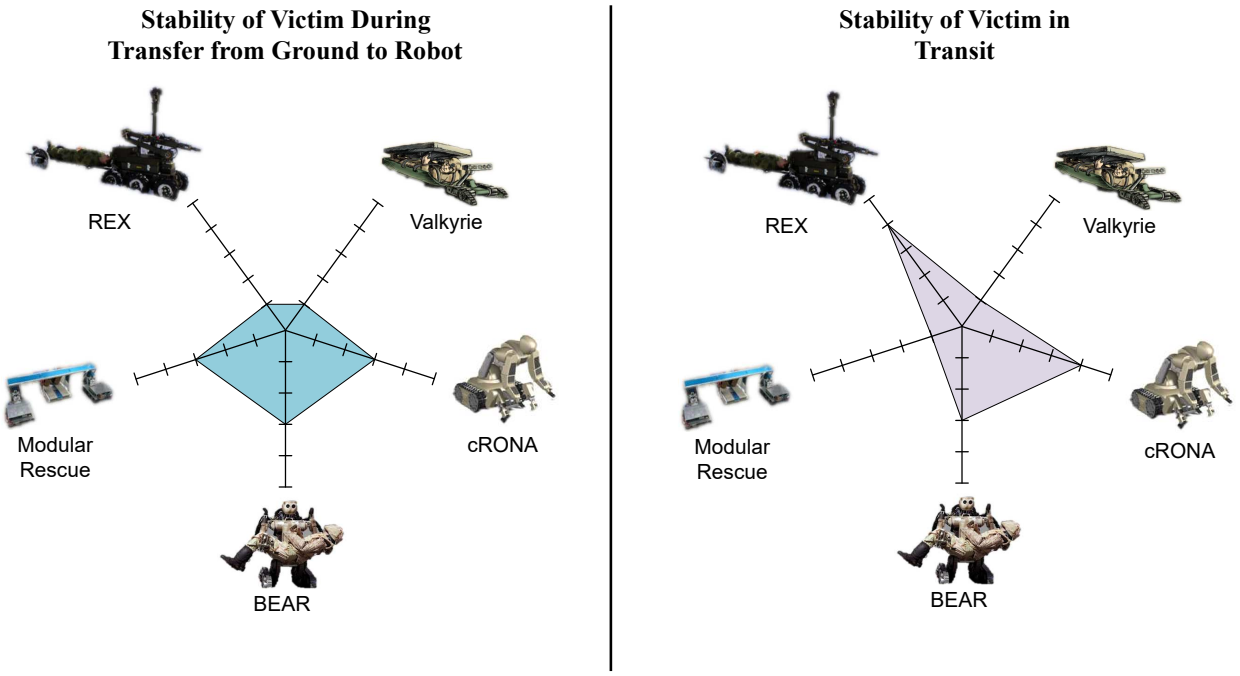

Figure 2.5: Graphical comparison of key extraction robot stability traits [7]

differences between the reviewed systems' ability to maintain stability of a transferred subject when transferring them onto the system as well as when transporting them to safety.

2.4 Evacuation Robots

Once an injured person has been safely extracted from the point-of-injury to a more secure location and first aid and/or triage has been conducted, the next step is often to transport them to a medical station for more in-depth medical attention. This stage presents an excellent opportunity for robotic assistance. To provide an improvement on the current methods, such a system would need to navigate to a medical station with some degree of

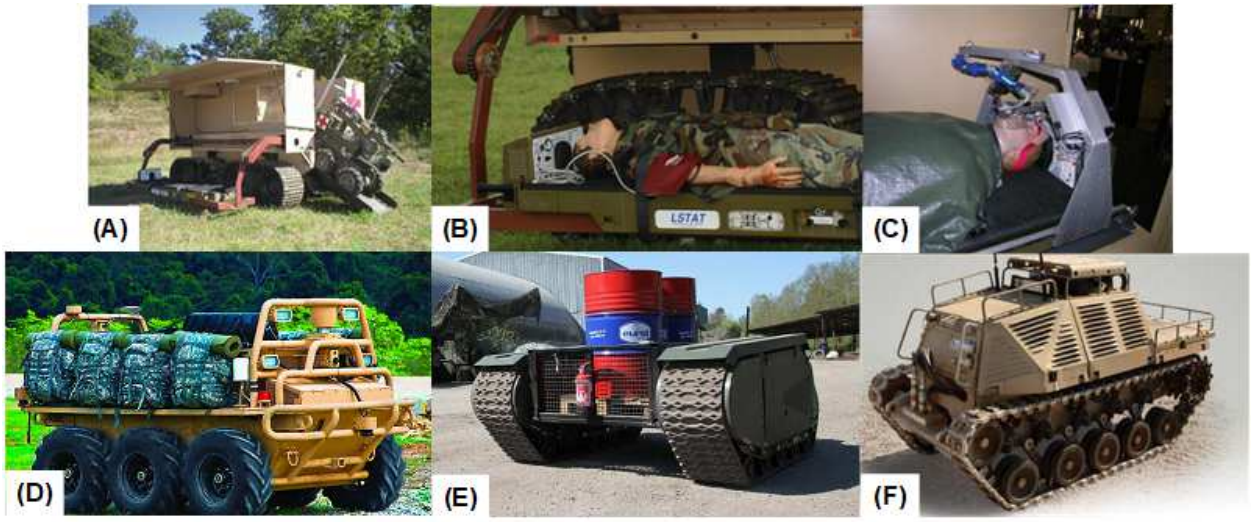

Figure 2.6: (A) REV [9] (B) LSTAT on REV [9] (C) LSTAT with Snakebot manipulator [9] (D) Lockheed SMSS [14] (E) Qinetiq Titan [15] (F) HDT Global Protector [16] [7]

autonomy while providing feedback on the injured person's current state. Research and development in this area has largely been focused on the creation of a larger, multi-purpose, mobile ground vehicle that has configurable modules to facilitate the evacuation of injured personnel and the peripheral systems intended to provide onboard patient monitoring in such operations [64]. The reviewed systems can be found in Fig. 2.6 below.

Robotic Evacuation Vehicle (REV): As previously described, the Robotic Extraction Vehicle (REV), is the larger transport half of the marsupial pair REX and REV. Upon reaching a combat zone, REV would deploy a ramp and send REX into the field to extract a wounded solider. Once retrieved, REV would act as an autonomous, reconfigurable transport vehicle equipped with two LSTAT stretchers and ballistic armor, in order to safely evacuate the wounded soldiers [38]. However, the U.S. Army did not allow autonomous transport of

wounded soldiers without a medic or attendant at the time when REV was being tested, so the design had to be reworked to incorporate a center module to provide for an on-board medic and allow for manual operation of the system [10]. An illustration of REV offloading REX in a field trial can be seen in Fig. 2.6A above.

Squad Multipurpose Equipment Transport: The Squad Multipurpose Equipment Transport (S-MET) program is a U.S. Army initiative intended to drive development of an autonomous or semi-autonomous mobile robot that transports the supplies required by an infantry squad to operate for 72 hours and provides a mobile power source to recharge the electronics carried by the soldiers [65]. These mobile robots would have manual operation, follow-the-leader, and autonomous navigation capabilities. In addition to the increased load carrying capabilities afforded by the S-MET, they must also be reconfigurable into casualty evacuation platforms, either through attachment points for a standard stretcher or through inherent medical transport capabilities [66]. Therefore, prior to entering a possible combat scenario, the squad could offload the supplies carried by the S-MET and convert it to casualty evacuation mode in order to create a standby evacuation vehicle.

The Lockheed S-MET model, the Squad Mission Support System (SMSS), is a field-tested mobile robotic platform that saw service by the U.S. Army in Afghanistan in 2012 [14]. The 4,300 lb. vehicle has the ability to pack stretchers on either side or in its bed when it is set up to perform casualty evacuation. In addition, it is capable of remote tele-operation as well as operating in a supervised autonomous mode.

A smaller S-MET design is the Titan Dismounted Troop Support System, built by Qinetiq

[15]. A simpler design than the SMSS, the Titan consists of a platform supported by two diesel-electric hybrid tracks, with mission specific controls and automation being contained in modular payload frames. One of the possible configurations includes stretcher racks that can be mounted on the robot, allowing it to easily transition from equipment transport to casualty evacuation vehicle.

A third S-MET is produced by HDT Global, called the Protector [16]. As with the previous versions, it is designed to transform into a casualty evacuation vehicle rapidly, with hard points built into the side to accommodate a folding stretcher. In addition, using ramps carried by the robot, a Protector can be driven directly onto a medical evacuation helicopter [67].

Life Support for Trauma and Transport (LSTAT): Once an injured person has been extracted from a dangerous area, there must be some manner in which to monitor his or her vital signs while being transported to receive further medical treatment. One such system is Integrated Medical Systems Inc.'s Life Support for Trauma and Transport (LSTAT) patient care platform [40]. While appearing to be simply a stretcher, it possesses enough capabilities to be considered a mobile ICU. The LSTAT system is made up of the stretcher itself, a ventilator, a defibrillator, a suction pump, a fluid and drug infusion pump, and a blood chemistry analyzer[68]. It also carries sensors that monitor blood pressure, pulse oximetry, end-tidal CO2, temperature, oxygen flow, and electrocardiography. The patient data is shown on a display mounted on the stretcher, and broadcast to a hand-held monitor or available wireless networks.

The LSTAT was well received in multiple field trials, both in hospitals and in military use. The in-hospital trials confirmed that the combined functionality was analogous to that provided by the multiple devices normally used to conduct this level of monitoring in hospitals [69]. In addition, the LSTAT was utilized successfully in aeromedical evacuation, by forward surgical teams, in amphibious assault vehicles, and in military support for civilian landmine victims [70]. By integrating so much monitoring ability, the necessary medical personnel for monitoring could be reduced in hospital and military scenarios.

The system was also envisioned as a key component intended to be integrated into the evacuation and treatment stages of the medical response process. For instance, REV was designed to accommodate two LSTAT stretchers. Once an injured person was placed onto the stretcher and monitoring was started, the stretcher could provide any medical personnel interacting with the patient detailed feedback on their vitals. In addition, its standard size would allow it to be transferred from evacuation vehicle to operating room to recovery, providing a continuity of monitoring and reducing the labor required (Palmer, 2010). Integration with the flexible Snakebot [46] was also explored to provide the LSTAT with a dexterous attachment [71]. This appendage could be used for multiple applications, ranging from actively inspecting the injured person for possible wounds to cauterizing hemorrhages utilizing short-range high intensity ultrasonic waves.

Over time, the LSTAT has been updated as the military has moved away from an integrated stretcher. Integrated Medical has since designed an updated device called the LS-1, billed as a “suitcase intensive care unit” [72]. Instead of the entire stretcher unit, the LS-1 contains

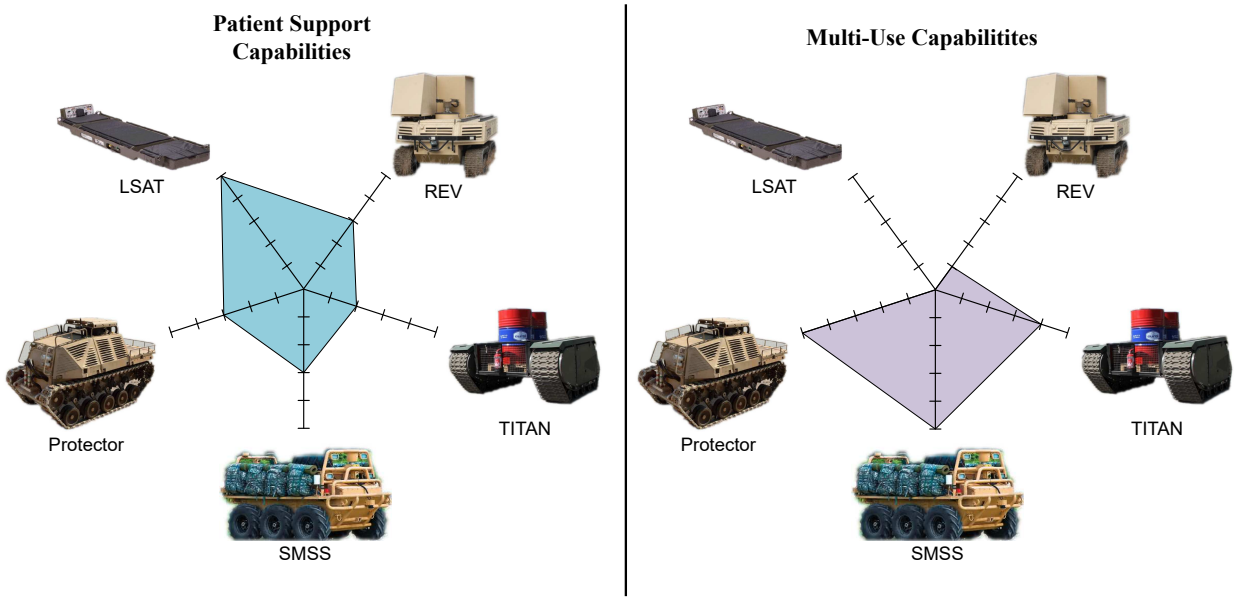

Figure 2.7: Graphical comparison of key evacuation robot capabilities [7]

the data acquisition capabilities from LSTAT in a package that can easily be clipped onto a standard military stretcher. This makes the unit even more portable and adaptable to the varied conditions that may be encountered in the field.

The evacuation systems described in this review possess many similarities, which is largely due to their military application. In disaster situations, the medical personnel are generally responding after the primary danger has subsided, and thus require shorter operating ranges for their equipment as medical treatment centers can be located near the disaster zone. A purpose built evacuation platform would not be used often enough to justify the inclusion of such a large piece of equipment in a squad loadout. Therefore, the overly specific REV has been supplanted by the more versatile pack mule-like S-METs. This provides operational flexibility while still providing evacuation capabilities if necessary. However, this removes

some of the patient-care specific benefits that REV incurred through the incorporation of the LSTAT into its design. The desire for a more compact and modular solution led to the creation of the LS-1. However, there is yet to be literature detailing the incorporation of LS-1 type monitoring devices into the S-MET type vehicles in order to provide medical monitoring. As such, the largest variations between these systems are in their capabilities to provide targeted patient support and their modular, multi-use capabilities. Figure 2.7 illustrates the difference in capabilities for the reviewed systems.

2.5 Field Treatment Robots

A challenge faced by many rescue operations is quickly allocating skilled medical personnel to the location of the incident, especially in remote areas. One way to alleviate this problem is to use systems intended to facilitate remote access to medical care. As mentioned previously, the initial research in this area led to the development of the Zeus and Da Vinci telesurgery robots [73]. While groundbreaking, these systems were too large to be easily incorporated into mobile operating settings. Research building upon these two systems has led to significant advances in field-applicable robotic surgical systems. The treatment systems graphically compared later in the thesis are seen in Fig. 2.8.

Current field medical robotic systems are focused on minimizing mechanical complexity while maintaining the necessary manipulability. The key to improving the feasibility of remote surgery is coupling the required minimal design with a control scheme designed to take

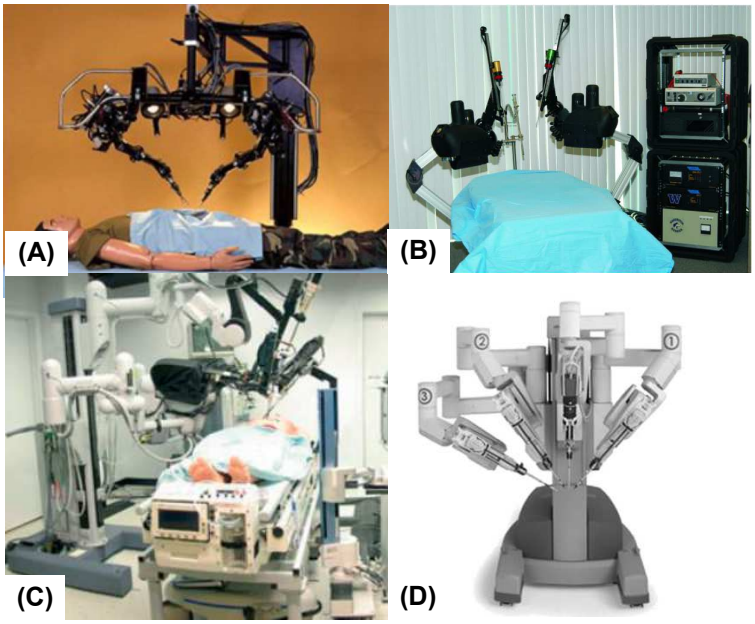

Figure 2.8: (A) SRI M7 [17], (B) RAVEN [18], (C) Trauma Pod [19] (D) Da Vinci [20]

into account the lag and intermittency that arise when using a remote video feed for direct operation. Both the SRI M7 and the RAVEN demonstrate the systems are fully capable of this task, by operating in remote fields, underwater, and even in free fall. However, they are experimental systems that have no yet fully tested. The Da Vinci, while a mature system, is too large and involves too much setup for portable usage as a standalone device, while the Trauma Pod would require a fixed base, like a large transport vehicle or drone in order to be used in the field. In Fig. 2.9, the applicability of the pictured systems for field usage is contrasted with the degree of clinical testing each has received.

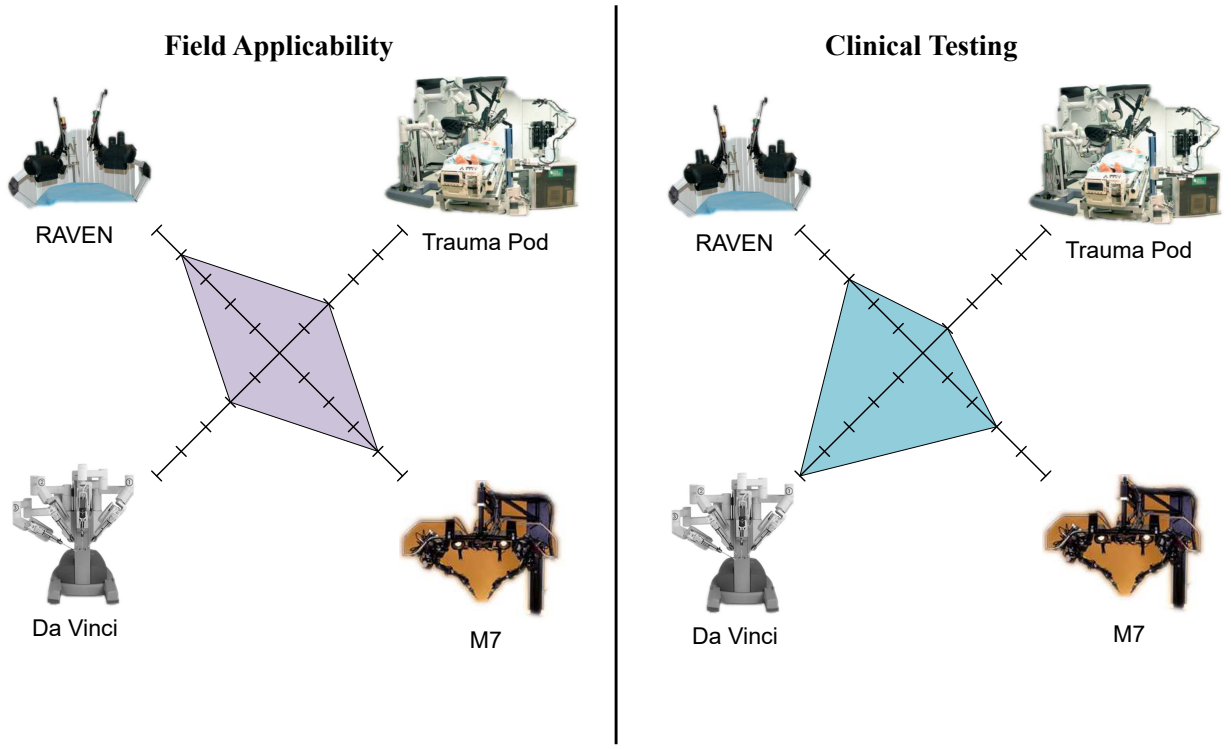

Figure 2.9: Graphical comparison of key treatment robot characteristics

2.6 Robotic Rescue Competitions

Developing the proper metrics for an accurate comparison for rescue robotics is often an extremely challenging task. The majority of the published work focuses only on how the proposed system will operate in a well-defined environment designed specifically for the intended problem. Since no clear criterion exists for the evaluation of these systems, the validation methods adopted by researchers vary greatly, making comparison of different systems solely based on published results nearly impossible. In this regard, robotics competitions are considered the major benchmarking method for field robotic systems, used as such because they provide objective classifications on how well a robot preforms a scored task [74, 75, 76].

Many major robotics competitions have featured "medical assistance and extraction" as the central theme, a part of their overall challenge, or as an event for demonstration purposes. Some of these competitions include The European Land Robot Trial (ELROB), euRathlon, RoboCup Rescue, and the Darpa Robotic challenge.

The RoboCup Rescue competitions were initiated as a part of the worldwide RoboCup competition in 2000 [77]. These include both the Rescue Robot League (RRL) and the Rescue Simulation League (RSL) [78, 79]. The events are designed to advance research in coordination of heterogeneous multi-agent systems. The Rescue Robot League involves exploring and searching for simulated casualties within an arena, including subtasks such as mapping, remote manipulation, and autonomous operations. The tasks, including the test environment, are based on the standard test methods for emergency response robots developed by the U.S. National Institute of Standards and Technology (NIST) [80]. This ensures that the tasks are conducive enough to drive academic research while representing capabilities in solving real-world challenges. In addition to the main event, teaching camps are organized as a part of the Rescue Robotics to help bring together best-in-class capabilities with the first responder community [81, 82]. Since 2016, the CarryBot league, which involves using robots that can transport material or even injured personnel in an outdoor scenario, has also been added . Even though the challenge is vastly simplified compared to real life situations, the competition is a major step towards creating interest among students and researchers in solving this problem. As the name indicates, the Rescue Simulation League focuses on designing intelligent behaviors for controlling and coordinating large groups of

robots through a single operator, and then testing them in a simulated environment. The operator provides high-level commands on areas to be surveyed and paths to be followed, and then supplies confirmations as necessary when detecting injured humans. Together, the robots create a shared map where all the sensor information is registered. In addition, there are events that compare the performance of algorithms that autonomously try to coordinate and control multi-functional teams in a simulated disaster scenario. The aim of Robocup Rescue is to advance the design of future rescue robots that are not just able to find the injured persons but also capable enough to free them from perilous situations.

DARPA started robotics competitions in 2004 with the Grand Challenge . The latest DARPA Robotics Challenge (DRC) had Urban Search and Rescue as the core theme. The DRC was directed at fostering research on robots capable of assisting humans in response to natural and man-made disasters. Inspired by the Fukushima Daiichi nuclear disaster, the competitions required humanoid robots to perform complex tasks like driving a utility vehicle, opening a door, handling valves, cutting holes in the wall, walking over piles of rubble, and climbing stairs and a ladder. For the finals that took place in June 2015, the tasks were made even more difficult by reducing the communication capabilities between the robot and the human operator. This enforced the need for perception and autonomy in the robots. In total, 23 teams participated in the event from different parts of the world, resulting in some of the most advanced humanoid rescue robots designed to date [83, 84, 85]. A major focus of the DRC was to develop ways to combine the complementary strengths and weaknesses of the robot system and human operator(s).

The EU-FP7 euRathlon project was a three-year initiative funded by the European Commission, started in 2013. As an international competition, it welcomes universities, industries, and independent teams from any EU country. The Grand Challenge, conducted on September 2015, was inspired by the Fukushima accident of 2011, providing real world challenges focused on outdoor robotics. The Grand Challenge required a collaboration of flying, land, and marine robots to survey the disaster area, collect data, search for missing workers, identify critical hazards, and work together to perform high level tasks such as closing valves in synchrony [86, 87].

The European Land Robot Trail (ELROB) is a robotics competition that has been running since 2006, focusing on military and civilian applications of advanced robotic systems, running on alternating years [88]. In recent competitions (starting in 2014), search and rescue scenarios such as locating injured personnel inside collapsed structures and performing medical evacuations (MedEvac) have been included in ELROB. During the 2014 and 2016 ELROB, many major institutions proposed solutions to the above issues. We will only discuss the major systems that were involved in the MedEvac challenge in this paper. For a complete review the reader may look into [89]. For the MedEvac challenge, two dummies representing wounded soldiers are hidden in non-urban terrain. Their approximate location was supplied to the team. The participant then had to locate the wounded 'soldier' and extract them to a base location, within a specified time limit. The 2014 ELROB MedEvac, hosted by Warsaw Military University of Technology and co-organized by Fraunhofer FKIE, had no penalties for damaging the dummy. Most of the teams had manipulators (such as Team Cobham and

ELP), but these were capable of handling only very small payloads. Therefore, most of the participants either used the manipulator to drag a dummy of reduced weight (Team Cobham and ELP) or used it to attach a hook to the dummy through teleoperation and then drag the dummy using the robot (Team FKIE). Other solutions included using lifting mechanisms (Team Oulu) or a forklift designed to lift heavy loads (Team Marek). Among the twelve teams that participated, only three were capable of locating and retrieving the dummies.

The MedEvac event gives participants the option of choosing the weight of the dummy they need to transport subject to penalties (70 Kg being zero penalties). During the 2014 event most of the teams opted for 10Kg dummy due to hardware limitations. However, in the 2016 ELROB all six participants were able to transport at least one of the full-size dummies for a short distance within the time limit. Three teams completed the full task of locating and extracting the two full-size dummies to the base location within the time limit. Despite major improvement compared to previous results, the transportation methodologies adopted by the teams were not practical when handling actual humans. Four teams (Team Kobra, Cobham, ELP, and Bebot) used a single manipulator and gripper to partially lift and drag the person back to the base. Team FKIE used the previous method of attaching a hook using the manipulator and then dragging the person on the ground. Team Avrora needed manual help in lifting the dummy and securing it onto the vehicle. In a real-life scenario, none of the above evacuation methods would be acceptable, which shows the amount of work needed in this area before robotic rescue and evacuation can be fully realized. The final ELROB is planned for 2018 at Riga, Latvia. Hopefully, this event will feature more mature designs

incorporating practical solutions that could be adopted for casualty evacuation in real life scenarios.

2.7 Conclusions Drawn from Literature Review

The maturity of search robotics means that many robust, field tested hardware designs are in use today. From the cases depicted above, several key conclusions can be reached. One of the most important is that search robots must be properly sized for their intended use, and that sizing is case dependent. For instance, several of the robots meant to be used at the World Trade Center after the September 11th attacks were too large for successful ingress into the nooks and crannies of the rubble. Another important takeaway from the literature was the benefit of a tether connection to the robot; both to ensure continuous communications and to use as a method of removal should the robot become trapped in a confined space. Finally, an effective mobile search robot is one that possesses the ability to adapt to the necessary terrain. From Soryu to Quince, this adaptability lends the robots the flexibility required for successful field deployment. Ongoing research in this area focuses on the use of these robots in autonomous and semi-autonomous multi-robot teams, in order to effectively search over a large area. Further work is required on methodologies and machine intelligence required for the robots to not only operate in tandem with other robots, but alongside search and rescue personnel with minimal training. Human-robot cooperation could vastly increase the usability and benefit imparted by search robots, and would help to

further their implementation by search and rescue teams world over.

In the area of casualty extraction robots, one of the critical challenges is keeping the injured person safe and secure during transport. One of the more difficult tasks in this operation occurs when attempting to transfer the injured or incapacitated person from the ground to the transport platform. By necessity, patient transfer requires some combination of lifting, dragging, or sliding, and current designs fail to place sufficient emphasis on maintaining a stable transfer mode. Further attention to this problem could reduce the danger of exacerbating any existing injuries or causing new ones. In addition, the existing systems all rely on direct, continuous operator control, which may face challenges when operating in remote locations with poor network infrastructure. A robotic platform with semi-autonomous communications and lag-compensating control, analogous to methodologies used in military drone flight, could help ensure the safety of the injured person when communications are intermittent.

In military use, purpose-built evacuation robots appear to have been replaced by modified multi-purpose transport systems. While repurposing robots results in a more efficient allocation of materials and resources, care must be taken that key functionalities are not neglected including autonomous patient monitoring and in-transit first aid. Integration of a system like the LS-1 into the transport configuration of an S-MET may be a good compromise between multi-purpose equipment and medical functionality. The dexterity and control of remote surgery systems has been steadily improving over the years. However, there are still facets of robotic surgery that require further attention, especially when considering field implemen-

tation. One such area is automated anesthesia. While there are extant robotic anesthesia systems [90], there has been no real push to create a field-usable version. In addition, the current systems have manipulators that can only work in the predefined workspace for which they are initially configured. In an emergency triage situation in a remote locale, surgical robots should be able to perform procedures on any location of the body without requiring human intervention to reposition the entire system. Such challenges are areas of current research, as further advancement is required before these systems can be implemented in a live operating theater in the field.

This comprehensive review of the state of the art in search and rescue robotics provide a through background and demonstrate the necessity of further research in this space. With this as motivation, work was conducted with the goal of designing a robotic rescue platform, capable of performing both the extraction and evacuation steps of the rescue process.

Chapter 3

Preliminary Design of the Robotic Head Stabilization System

3.1 Semi-Autonomous Victim Extraction Robot (SAVER)

The prior technical background demonstrated the uses and extant needs in a robotic rescue platform. In collaboration with RE^2 and the US Army Telemedicine and Advanced Technology Research Center (TATRC), research into the design requirements for a next-generation casualty extraction robot was initiated. A preliminary design concept for a Semi-Autonomous Victim Extraction Robot (SAVER) [91] is shown in Fig. 3.1. This thesis focuses on the head support subsystem shown in the figure.

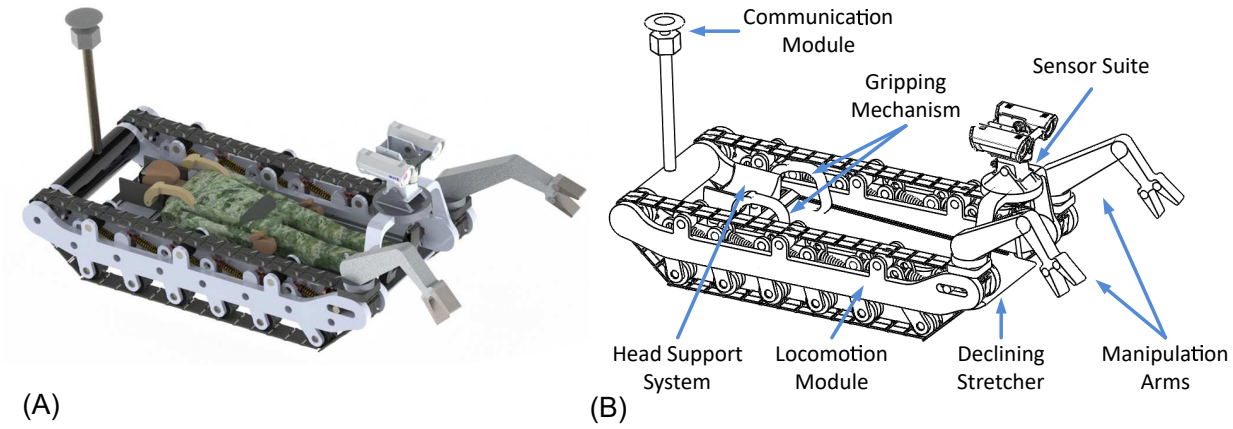

Figure 3.1: Preliminary design of SAVER

3.2 Motivation for Head Stabilization on SAVER

Traumatic injury can often result in dangerous and even fatal damage to the spinal cord, with 20% of such injuries resulting in fatalities before patients are even admitted to a hospital [92]. In cases that do not result in fatalities, spinal injuries can result in paralysis, chronic pain, and long-term hospitalization. When assisting trauma patients, first responders take extensive precautions to minimize head motion in order to prevent further damage or injury to the spinal cord in the neck (cervical spine).

In the 2002 Guidelines for the Management of Acute Spine and Spinal Cord Injuries, published by the American Association of Neurological Surgeons, the recommended procedure for all cases in which a cervical spinal injury is suspected is to stabilize the patient using "a cervical collar and supporting blocks" [93]. Figure 3.2 demonstrates standard neck stabilization and immobilization.

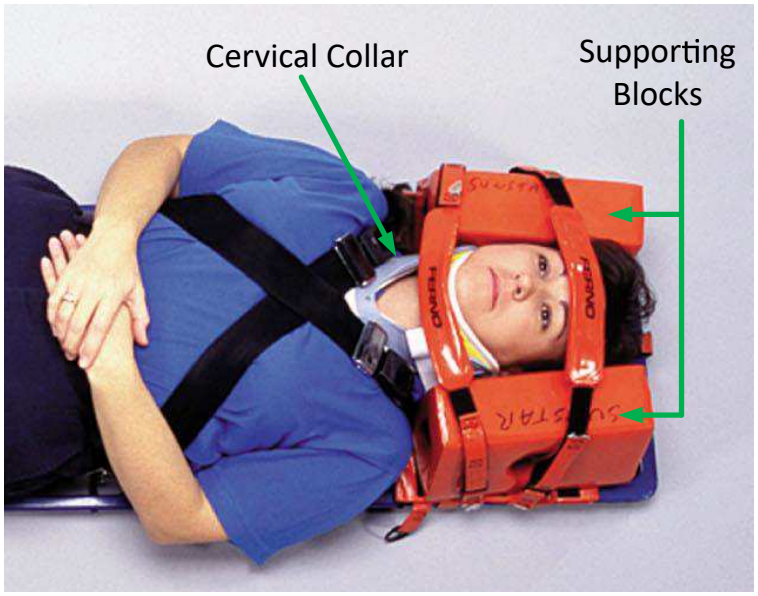

Figure 3.2: Example of Standard Neck Stabilization and Immobilization [21]

The Emergency Medical Technician (EMT) National Curriculum concurs; recommending a standard procedure should the responding EMTs suspect the patient has suffered a neck injury. The procedure is as follows [25]:

1. The neck should be manually stabilized in-line with the spine.
2. A rigid immobilization device (i.e. cervical collar) should be applied.
3. The head and neck should be stabilized using supporting blocks, sand bags, or similar devices

However, despite the recommendation that cervical collars be applied only when a cervical spine injury is suspected, in common practice rigid collars are often applied to all trauma patients regardless of the presence of a suspected neck injury.

Recent research has shown higher than expected rates of complications associated with unnecessary use of rigid cervical collars, such as ankylosing spondylitis(an arthritis of the spine), increases in intracranial pressure resulting in head injury, compromised airway management, and delayed resuscitation of patients with penetrating trauma [94]. This has sparked extensive work investigating the benefits and the hazards of the use of such collars [26, 95]. The research has led to new guidelines and procedures for the neck stabilization, calling for reduced and more discretionary use of rigid cervical collars in trauma situations [96], with some suggesting an algorithmic evaluation of the injury severity to determine the necessity of spinal immobilization [97, 98]. Other researchers have questioned the benefits of any immobilization, finding fewer complications in foreign hospitals that do not practice pre-hospital immobilization [99].

However, there are still benefits to be gained through the use of some measure of stabilization for a patient who has suffered a traumatic injury. Should critical damage be present in the cervical spine, further motion could cause further injury or death. Research has shown that cranio-thoracic stabilization methods such as sandbags or stabilization blocks upon a stretcher can nearly completely stabilize the cervical spine, without the use of a cervical collar [100]. This thus forms the basis for the necessity and function of the proposed head stabilization device. Due to the uncertain benefits of rigid collar application and the requirement of case-by-case evaluation for its use, automated cervical collar application strategies were not be considered in the head stabilization device.

A major design goal for the subsystem was to have the two supporting blocks driven by a

single actuator. Each block will maintain the freedom to reach an asymmetric final position, while applying constant force to hold the head steady without causing discomfort. The allowance of an asymmetric final position gives the device the ability to stabilize the head and neck in the position in which the patient is originally encountered or in the position in which it is manually placed by a trained emergency medical professional. In addition, the asymmetry helps the device to better accommodate patients wearing headgear or helmets. An asymmetric final position is achievable through incorporation of a differential mechanism, which applies a single input to two or more outputs independently. Therefore, the use of this subsystem as designed would result in the patient being protected against further injury from excessive motion of the head, and the potentially injurious effects of unnecessary in-line stabilization could be avoided.

When evaluating the benefits of the subsystem as a standalone device, an important statistic to consider is the mean time for neck stabilization by medical first responders, which was found to be 5.64 min +/- 1.49 min [101]. The incorporation of an automatic head stabilization subsystem into standard first responder equipment could decrease that time, an important benefit in a life-saving scenario. In addition, automatic active stabilization removes the necessity for a medic to manually stabilize the head continuously until a cervical collar is correctly applied when deemed necessary by the medical responders. This would be an especially valuable benefit for two-man first responder teams by making that medic available to do other critical tasks [102].

Various differential mechanisms were analyzed in order to determine the design benefits

incurred from the use of such mechanisms. To quantify the comparison process, a static analysis similar to that performed by Birglen and Gosselin in [103] was incorporated. In order to provide analysis for simulation and controller design via force analysis in multiple operation modes, a dynamic simulation derived through first principles and geometric analysis of the mechanisms was performed. The design for the robotic head stabilization device then incorporated the most mechanically advantageous mechanism.

3.3 Prior Work

Few projects have investigated robotic stabilization of the head in rescue situations. A study was conducted by Yim et al. on the use of a foam based stabilization system for a modular rescue robotic system, where a foam gel was sprayed by a robotic module around the patient's head and allowed to set in a cardboard mold [104]. While the foam provided good support, it required a set amount of time to harden around the patient's head. After transport, the foam would often stick to the head of the patient, requiring it to be broken or cut off. While a flexible and customizable support, these drawbacks make foam gel a less than ideal head stabilization method.

The MechaNek is a head stabilization device designed to protect professional race car drivers in crashes [105]. As an upgrade to the Head and Neck Support (HANS) device worn by motorsports drivers, it is intended to clip to a helmet and hook onto the driver's shoulders to provide stability during crashes. Actively actuated cables are connected between the

shoulders and head, keeping constant tension but allowing the driver to utilize the full range of motion of their neck. This is an upgrade over the fixed cables of the HANS. By interfacing with the car's onboard computers, the MechaNek will restrain the head when an imminent crash is detected in order to prevent traumatic spine injury. However, this device is solely intended for use as a portion of the protective equipment worn by motorsports drivers and alternative applications have not been described.

3.4 Differential Mechanism Analysis

As defined by Hirose in [106], a connected differential mechanism is one in which the dynamic inputs to the mechanism are balanced between multiple "ports," or degrees of freedom (DOF). Ccommonly encountered examples are shown in Fig. 3.3, including a fluid filled t-pipe, a sliding pulley, a sliding seesaw, and variations of gear-based systems. An easily recognizable differential mechanism is the bevel gear differential found on the drive axle of an automobile. The most common usage of these devices in robotics is in underactuated robotic hands, prosthetics and exoskeletons; sliding pulleys are used in [107, 108, 109], differential levers in [110, 111, 112], and a planetary gear differential in [113].

The driving motivation behind the proliferation of differential mechanisms in robotic hands is the grip adaptability afforded by differential mechanisms, both in terms of compliant finger position and in grip force distribution [114]. In addition, multiple differential mechanisms can be operated in serial and parallel combinations, granting greater flexibility of grip and a

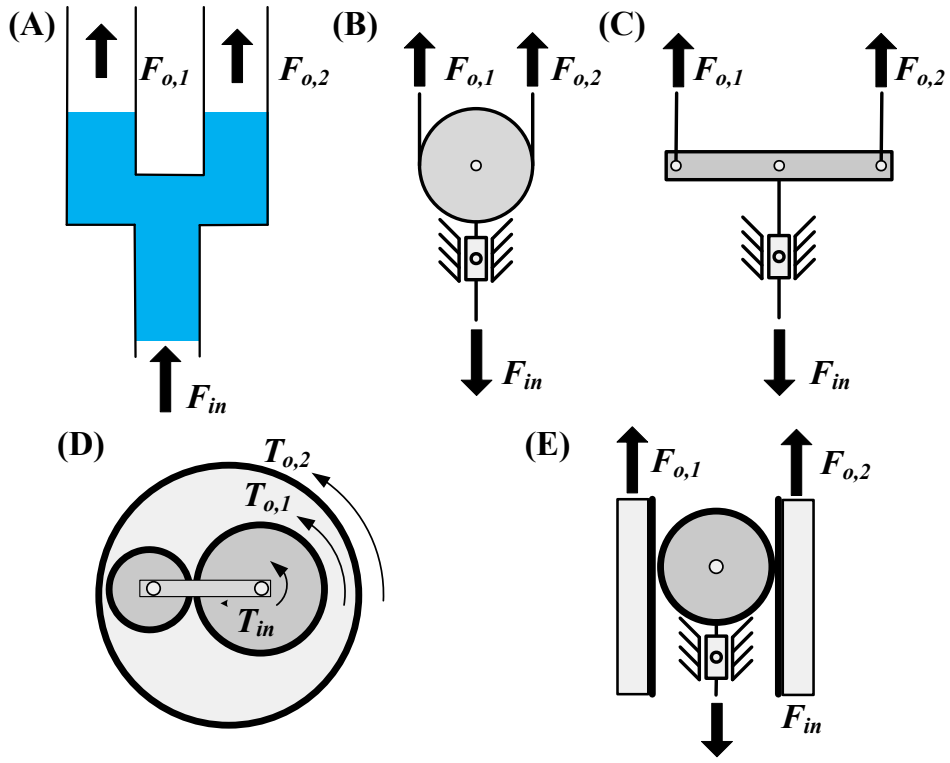

Figure 3.3: Various types of differential mechanisms [22]

closer approximation to experimentally recorded common grip postures, sometimes referred to as synergies [115]. Through application of different versions of differential mechanisms, the input forces and/or displacements can be distributed equally throughout the output channels, such as in [107] and [109], or may be preferentially distributed by selectively varying the geometry of the mechanism such as in [110] and [111]. The non-uniform distribution is often due to the design goal of attributing greater grip force to the thumb in comparison to the force at each of the four remaining fingers.

Furthermore, the ability to couple multiple DOF to a single actuation point greatly reduces the required actuation density for the design. This is of considerable advantage when creating

a small form factor device that contains many DOF. As mentioned previously, prior work concerning static force analysis of single and cascading differential devices as well as the desired cable configuration for differential planar manipulators has been conducted by Birglen and Gosselin, Baril et al., and Khakpour et al. in [116, 103, 117]. While similar equilibrium force analysis is contained here, additional investigation was merited in order to demonstrate the benefits of the respective mechanisms to choose the most advantageous configuration for the robotic head stabilization subsystem.

For the stated goals of this device, several differential mechanisms can be immediately discarded from consideration. The fluid pipe configuration is undesirable due to the required inclusion of a compressor or pump as well as the risk of leaks. In addition, the gear-based systems necessitate adequate lubrication and require precision manufacturing, increasing the cost to incorporate them into a design. The remaining mechanical devices, the sliding pulley and seesaw, are excellent prospective components. Both combine simplicity of fabrication with similar actuation requirements, leading to analogous static and dynamic data for a straightforward performance comparison. Therefore, these two mechanisms are focus of the following analyses.

3.4.1 Pulley Static Analysis

A free-body diagram of a sliding pulley with diameter R can be seen in Fig 3.4. In the system, the pulley would be mounted on a prismatic joint at its center revolute joint, allowing it to

translate in both the positive and negative y-direction. The force F_in is then applied to the pulley center, creating the resultant output forces $F_{o,1}$ and $F_{o,2}$. These two output forces are equal to the tension forces in the cables. Due to the rotation θ of the pulley to balance the moments applied, the cable angles α_1 and α_2 with respect to the horizontal axis remain constant values.

When in equilibrium, the forces on the mechanism can be determined by moment and force balance. The relation between the output forces and the input forces can then be calculated giving Eq. 3.1 and Eq. 3.2.

$$F_{o,1} = \frac{F_{o,2} \sin \alpha_2}{\sin \alpha_1} \tag{3.1}$$

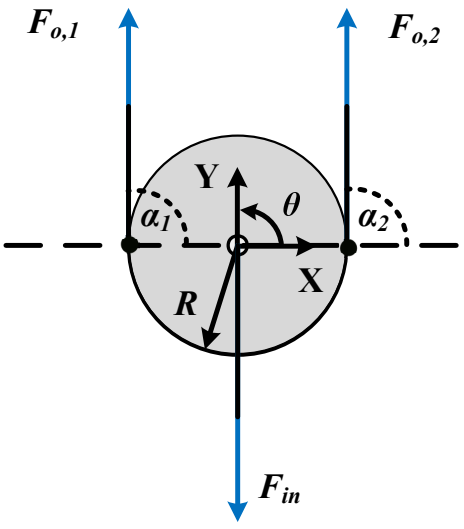

Figure 3.4: Sliding pulley free-body diagram [22]

$$F_{o,1} = \frac{-F_{in}}{2\sin\alpha_2} \tag{3.2}$$

The force relations show that the output forces are inversely proportional to the initial angle α_i. It can also be seen that if $\alpha_1 = \alpha_2$, the two forces will always be equal in equilibrium. When $\alpha_1 = \alpha_2 = \frac{\pi}{2}$, the two output forces will both be $\frac{-F_{in}}{2}$. While an initial angle less than $\frac{\pi}{2}$ would result in greater tension forces, the angles would then be proportional to the varying y-displacement of the pulley as the geometry of the system changes. To avoid this, in further analyses of the sliding pulley $\alpha_1 = \alpha_2 = \frac{\pi}{2}$ is chosen to be the initial angle.

3.4.2 Seesaw Static Analysis

Free-body diagrams for the sliding seesaw of length $2L$ are shown Fig. 3.5 below, with the pulley at its initial state (A) and after translation and rotation due to asymmetric contact with the head (B). The beam possesses a revolute joint at its center, which would in turn be mounted on a prismatic joint to facilitate translation of the seesaw in the y-direction. An input force F_{in} is applied in the negative y-direction along the prismatic joint. The device will thus transfer its force and inputs to the two output forces$F_{o,1}$ and $F_{o,2}$. Should one block contact the head before the other, the seesaw will rotate about its central revolute joint by an angle θ until equilibrium is achieved. For the two cables, the angle from the vertical is denoted by γ_1 and γ_2.

The angles γ_1 and γ_2 can be calculated using Eq. 3.3 and Eq. 3.4, respectively

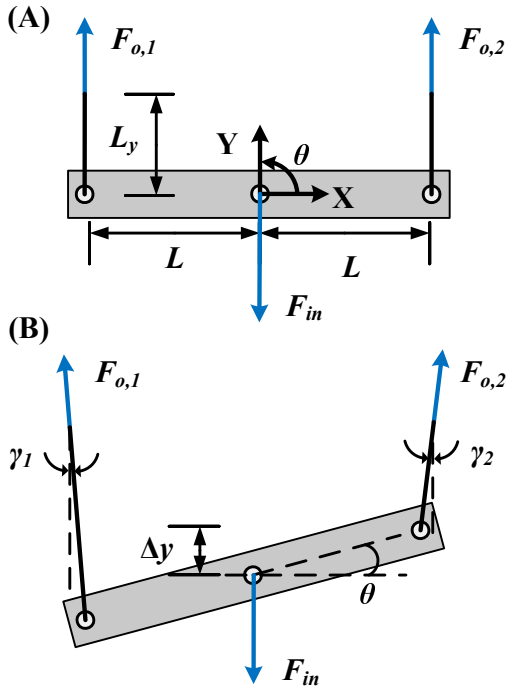

Figure 3.5: Sliding seesaw free-body diagram: (A) Initial position (B) Position post rotation and translation [22]

$$\tan\gamma_1 = \frac{L - L\cos\theta}{L_y - \Delta y + Lsin\theta} \tag{3.3}$$

$$\tan\gamma_2 = \frac{L - L\cos\theta}{L_y - \Delta y - Lsin\theta} \tag{3.4}$$

where L_y is the initial vertical cable length and Δy is the vertical displacement of the seesaw along the prismatic joint. In combination with force and moment balance on the mechanism, Eq. 3.3 and Eq. 3.4 can be utilized to give the individual force relations in Eq. 3.5 and Eq. 3.6.

$$F_{o,1} = \frac{F_{o,2} \cos \gamma_2}{\cos \gamma_1} \tag{3.5}$$

$$F_{o,2} = \frac{F_{in}}{2 \cos \gamma_2} \tag{3.6}$$

It can thus be observed that the seesaw's two force outputs vary independently with θ due to the asymmetry of γ_1 and γ_2. Again, the redirection pulleys will be placed directly above the beam's cable connection points in order to avoid a dynamically varying initial angle offset.

3.4.3 Pulley Dynamic Analysis

For the pulley system, the equations relating the motion of the pulley to the forces applied can be found through a geometric analysis of the system. The pulley output cables are wrapped around redirection pulleys to transfer the vertical translation of the sliding pulley to horizontal translation of the supporting blocks. Frictionless rotation with no slip is assumed in all three pulleys. In order to detail the motion that occurs once the right supporting block has made contact with the asymmetrically located head of the patient, the corresponding cable will be treated as if it terminates at a fixed point. The spring component due to the block's compliant foam composition is assumed to be trivial.

A diagram showing the resultant system is shown in Fig. 3.6, where y is the vertical distance from the pulley starting point, and x is the horizontal distance from the unfixed block's original position. As stated previously, the initial angles between the output cables and the

horizontal axis are assumed to both be $\pi/2$. Due to this symmetry, the two output forces will always be equal, and are represented by F_o.

The cable from one block to the other is observed to be of constant length. By differentiating the sum of the components with respect to time, the relation between y and x is found to be $\ddot{x} = \frac{-\ddot{y}}{2}$ Application of this relation along with force summation at the pulley and block results in Eq. 3.7, representing the vertical acceleration and Eq. 3.8 representing the cable tension.

$$\ddot{y} = \frac{F_{in}}{4m_b + m_p} \tag{3.7}$$

$$\ddot{y} = \frac{-F_{in}}{2 + m_p/2m_b} \tag{3.8}$$

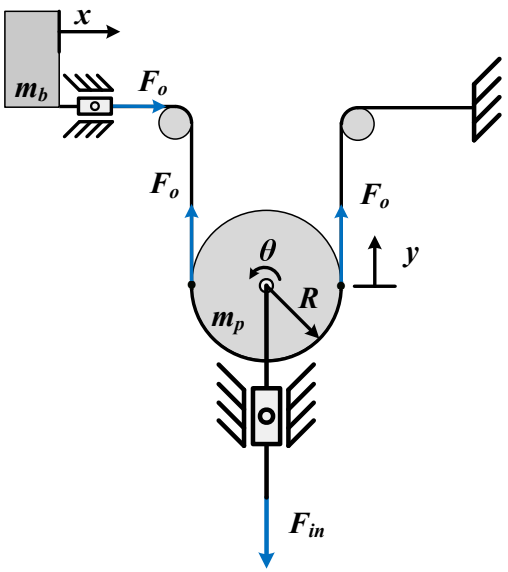

Figure 3.6: Fixed cable sliding pulley diagram [22]

where m_b is the mass of the supporting block and m_p is the mass of the pulley. Note that F_o is independent of the system's motion in this case. The fixed-point assumption holds so long as the tension force F_o is less than the static friction force at the patients head, $m_h g \mu_s$ where m_h is the mass of the head, g is gravitational acceleration, and μ_s is the static friction coefficient.

In addition, the angular acceleration of the pulley is found through the relation between tangential and angular acceleration, $\ddot{y} = R\ddot{\theta}$. Utilizing this and the above equations, a dynamic model of the system was written in MATLAB. Fig. 3.7 depicts the behavior of the system when the mass of the pulley, m_p, is 0.1 kg, the radius of the pulley, R, is 0.1 m, the mass of the supporting block, m_b, is 2 kg, and a constant force, $F_i n$, of 0.5 N is applied in the negative y direction.

As depicted in Fig. 3.7, the support block on the right remains fixed. The induced rotation in the pulley due to the fixed constraint results in the translation of the left block in the positive x direction. The dynamic model reinforces the expected motion of the system.

3.4.4 Seesaw Dynamic Analysis

Applying similar geometric analysis methods as in the previous section lead to the equations describing the motion of the seesaw after the supporting block on the right has contacted the patients head. Again, the block on the right is replaced with fixed cable termination, the pulleys' motion is assumed to be frictionless, and the spring component in the block

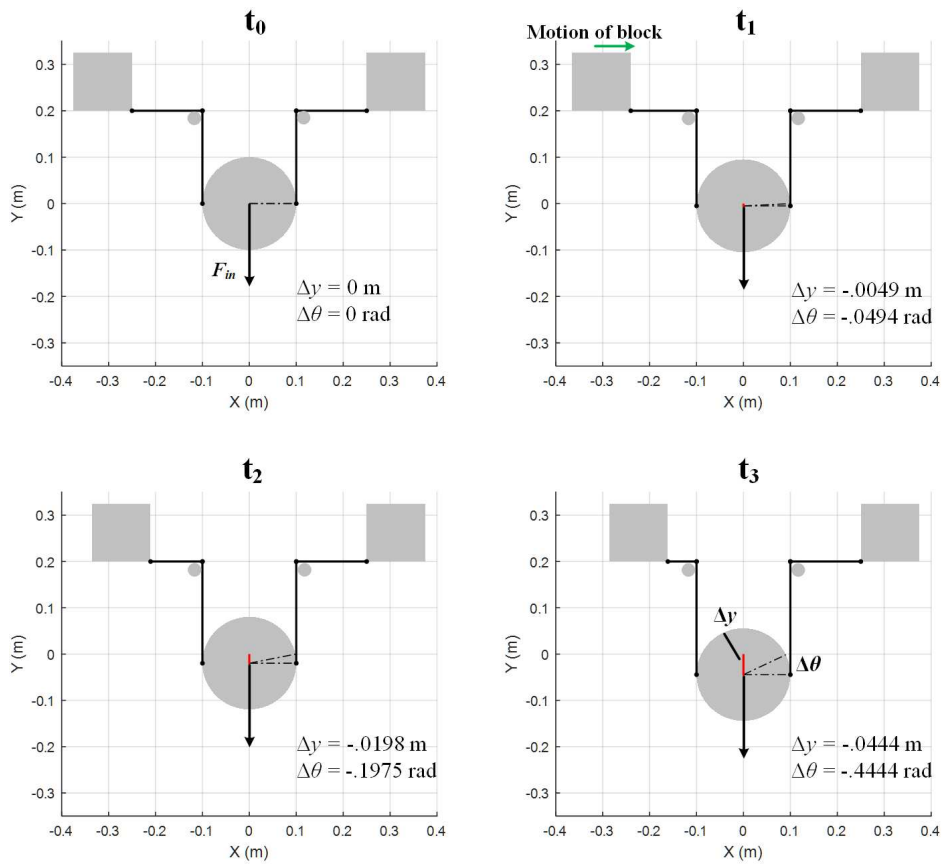

Figure 3.7: Dynamic model of sliding pulley system [22]

in contact with the head due to the block's compliant foam composition is assumed to be trivial.

The resultant system is seen in Fig. 3.8. The cable tension of the cable connected to the moving block is denoted by $F_{o,1}$, while that of the fixed cable is $F_{o,2}$. As with the pulley, the input force is represented by F_{in}. In the diagram, y is the vertical distance from the initial seesaw position, and x is the horizontal distance from the moving block's original position. The seesaw mass is represented as m_s and the supporting block mas is m_b. The seesaw is depicted a short time after the right block has contacted the person's head in order to

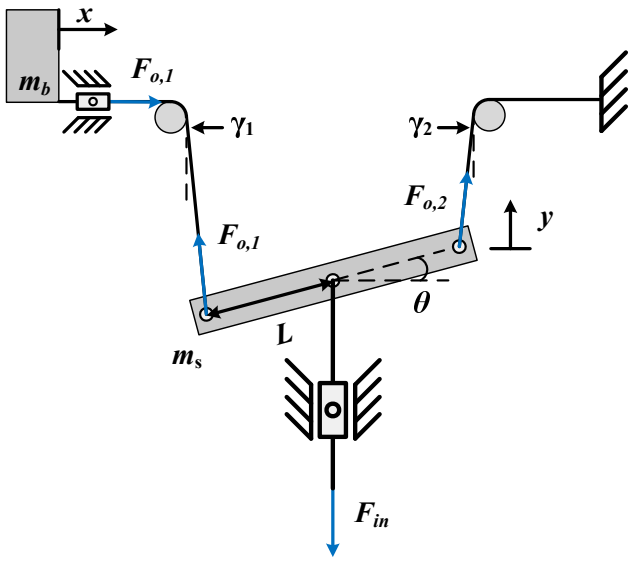

Figure 3.8: Fixed cable sliding seesaw diagram [22]

demonstrate a small degree of rotation and the corresponding configuration.

The cable from the connection point on the left side of the seesaw to the supporting block is a fixed length. By differentiating the sum of the components of the cable, the relation between linear and rotational acceleration is found to be $\ddot{x} = -\ddot{y} - \ddot{\theta}L\cos\theta + \dot{\theta}\cos\theta$. This can be combined with the results of the force balance of the beam and block to derive the equations of motion. The vertical acceleration is calculated by Eq. 3.9 and the rotational in Eq. 3.10. In order to linearize the equations, small angle approximations were applied for appropriate instances of γ_1 and γ_2.

$$\ddot{y} = \frac{-F_{in} + F_{o,1}(1 + \gamma_1/\gamma_2)}{m_s} 55 \tag{3.9}$$

$$\ddot{\theta} = \frac{-F_{in} + F_{o,1}(1 + \gamma_1/\gamma_2)}{L m_s \cos\theta} + \dot{\theta}\tan\theta^2 \tag{3.10}$$

The tension forces $F_{o,1}$ and $F_{o,2}$ can be calculated with Eq. 3.11 and Eq. 3.12, respectively, through the differentiation of the relation between the static cable length of the fixed side and the displacement of the seesaw center, y.

$$F_{o,1} = \frac{F_{in}\gamma_2}{m_b(m_s - 1)(\gamma_1 + \gamma_2) + \gamma_2 m_b} \tag{3.11}$$

$$F_{o,2} = F_{o,1}\frac{\gamma_1}{\gamma_2} \tag{3.12}$$

As with the pulley, the fixed-point assumption holds so long as the tension force $F_{o,1}$ is less than the static friction force applied to the patients head, $m_h g \mu_s$ where m_h is the mass of the head, g is gravitational acceleration, and μ_s is the static friction coefficient.

Using the above equations, a dynamic model of the system was created in MATLAB. The results of a simulated system are shown in Fig. 3.9, where the mass of the pulley m_s is 0.1 kg, the mass of the block m_b is 2 kg, the pulley half-length L is 0.1 m, and the applied force F_{in} is 0.5 N in the negative y direction.

In the results above, the right block remains statically fixed, as shown in Fig. 3.8. When a downward force is applied, the cable constraint on the right side induces a counterclockwise rotation. The rotational motion and the vertical displacement result in the horizontal

translation of the left block. The results of the dynamic model correspond to the expected behavior of the system.

3.4.5 Design Analysis Conclusions

Several conclusions on the merits of the respective differential mechanisms can be reached through consideration of the results of the prior analyses. Due to the inherent rotation in

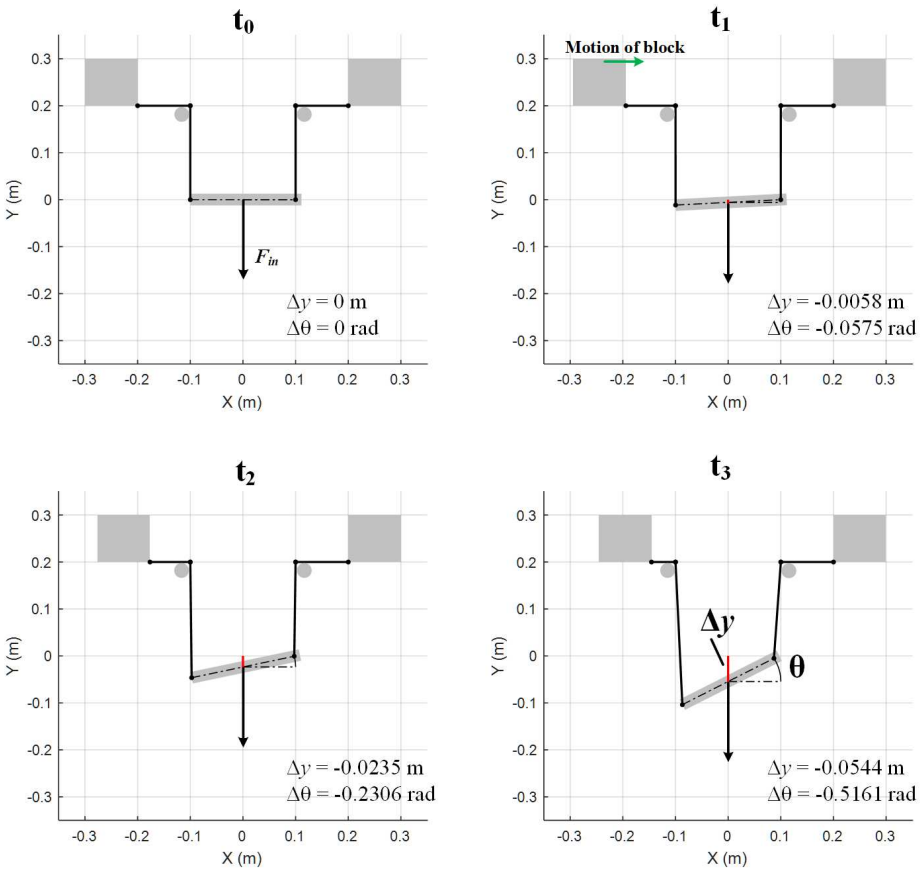

Figure 3.9: Dynamic model of sliding seesaw system [22]

order to balance the applied moments, the output forces of the pulley are independent of its angle of rotation, θ. In contrast, the seesaw's forces vary with the change in angle γ_1 and γ_2, which are in turn a function of the angle of rotation. In addition, the seesaw can allow for a maximum misalignment of $2L \sin \theta_{max}$, where θ_{max} is the angle of rotation at which the seesaw is in line with the fixed cable and is a function of the vertical length of the cables as well as the length of the seesaw. Due to this constraint, the seesaw must be sized to have a length proportional to the desired misalignment. In contrast, the amount of misalignment allowed by the pulley is limited only by the total length of the cable. Thus, a much smaller pulley can provide the same degree of compliance as a large seesaw.

In summary, it can be concluded that for the purposes of a compliant head support device the most advantageous differential mechanism is a sliding pulley. The sliding pulley will translate along a low friction linear motion carriage mounted on a lightweight aluminum track. The supporting blocks will also be mounted on low friction carriages that translate on an aluminum track perpendicular to that of the sliding pulley. Additionally, the supporting blocks will have small rollers on their base to help facilitate sliding when being translated. A system schematic and an example of its operation with an asymmetric head location can be seen Fig. 3.10. This configuration has been chosen in order to provide a clear view of the system operation from an overhead view, however future work will involve the optimization of the configuration with an emphasis on compactness and portability.

The redirection pulleys can be optimized to reduce the required range of motion for the sliding pulley. Instead of a single pulley, a two-tiered dual-diameter pulley can be used.

The cable on the smaller diameter will be connected to the sliding pulley, while the larger diameter will be connected to the blocks. This applies a gear reduction proportional to the ratio of radii, $n = R1/R2$, so that at the cost of increased input force, the linear motion of the sliding pulley is multiplied by a factor of n when redirected to the supporting blocks. In order for the blocks to return to their starting location, constant force springs will be connected to the blocks' roller carriages and to the end of the track. This low force will be easily overcome by the motor, but when the system is put into reverse the force will provide enough tension to pull the blocks back to their original position. An actuation unit containing the motor and controller will be mounted behind the pulley.

As mentioned previously, the head stabilization subsystem is intended to function both as a standalone device and as a sub-system on a mobile stretcher robot. In standalone form, the device would be portable, allowing a medical responder to bring it to the location of the injured person. If the medic deems it necessary, he or she could align the patient's head in a more advantageous position. Then the system would be activated and the supporting blocks would gently make contact with the patient's head, holding it in place with constant force.

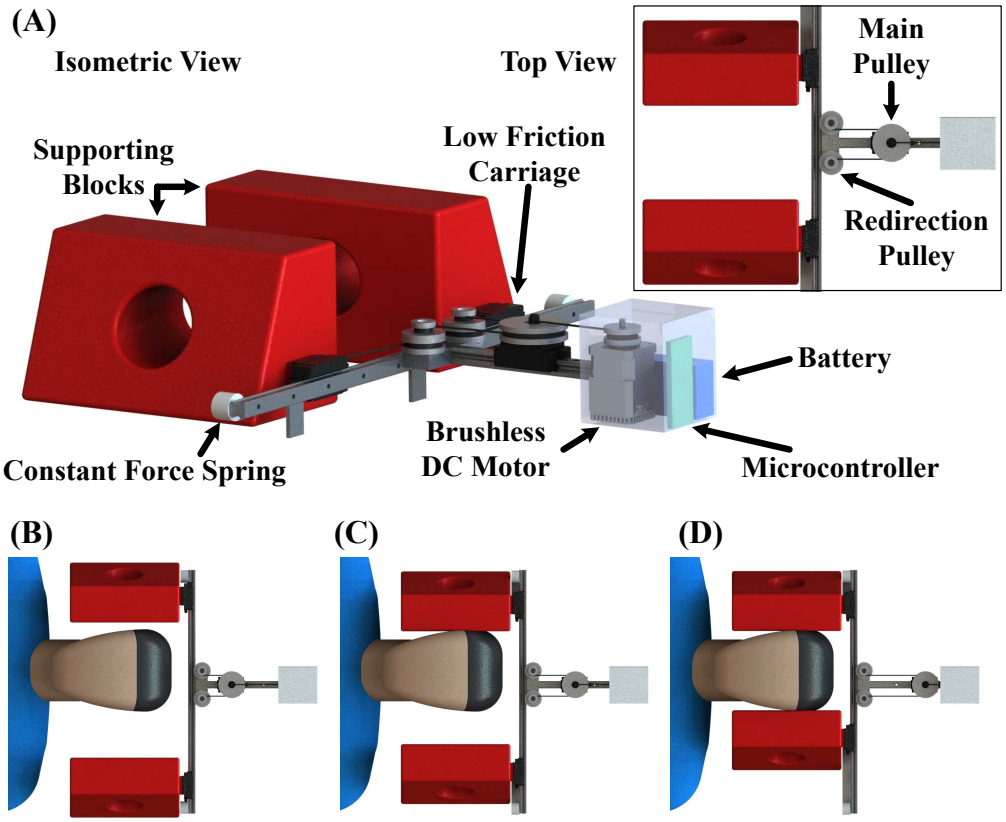

Figure 3.10: A) Robotic head stabilization subsystem with inset top view (B)-(D) System operation with an asymmetric head location [22]

Chapter 4

Control of the Preliminary Head Stabilization Device

When considering the manner in which to control the device, pure position control of the driving pulley is an inadequate approach as it may try to force the injured person's head into an undesired posture, without considering any existing injuries or complications. A better approach is to stabilize the victim's head and neck in the position in which the patient is originally encountered, while applying a constant supportive force. Relying on the differential mechanism to provide position compliance, the control system is required to apply a stabilization force within the safe threshold. The system needs to be designed such that under the presence of both position and force disturbances the head blocks should not exert a support force exceeding the set limit.

Force control is done typically using a high quality servomotor coupled with a feedback control algorithm using a stiff load cell [118, 119, 120]. However, for the above-mentioned application this method has several shortcomings [121], including the fact that direct drive actuators of desired torque and speed characteristics would be bulky and expensive. The resulting head support subsystem would be too heavy to transport and too expensive for general use in disaster zones. Smaller servomotors with gear reduction, such as the Firgelli linear actuator that was used in this design, introduce significant friction and inertia, reducing the force fidelity of the entire system. Moreover using stiff load cells for force feedback introduces chatter, resulting in sluggish control schemes. In addition, the non-uniform geometry of the human head and clinical requirements of replaceable or serializable head support blocks precludes straightforward measurement of the applied force at the contact point between the head and the support block.

Based on the above requirements the best approach would be the use of a series–elastic actuator (SEA) [122, 121]. The SEA design counteracts the above shortcomings by integrating an elastic element for force measurement and compliance. Similar to the load cell method, SEAs use active force sensing and closed loop control to counteract the effects of friction and inertia. However, force feedback is achieved by directly measuring the compression of the compliant element. A feedback controller calculates the error between the actual force and the desired force, applying appropriate control action to reduce the force error. The advantage is that SEAs introduce significant compliance between the actuator's output and the load, allowing for greatly increased control gains, while still ensuring the absence of chatter

and stability. This results in high quality force control with smaller, low precision actuators without the use of expensive load cells.

For the initial head stabilization device, the driving pulley was actuated by a linear actuator through an extension spring. A linear potentiometer will be used to measure the extension of the spring. As mentioned previously, constant force retraction springs will be used to bring the head support blocks back into the starting position when the force on the driving pulley is released. Studies performed on the actuation effect of the muscles anchoring the cervical spine show a force of around 16 N perpendicular to the spine corresponds to approximately 35° of rotation [123]. Thus, the system will be designed along these metrics, with a desired force of 10 N to be applied to each side of the head of 10 N, for a total support force of 20 N. A line diagram depicted the representative forces is shown in Fig. 4.1

If the force exerted by the driving pulley is known, the force exerted on the head by the support blocks can be obtained by taking the force balance at the head support blocks and the driving pulley:

$$f_h(t) = \frac{fin(t)}{2} - f_c \tag{4.1}$$

4.1 PID Model for Preliminary Design

In order to design the force controller, the following assumptions were made regarding the subsystem:

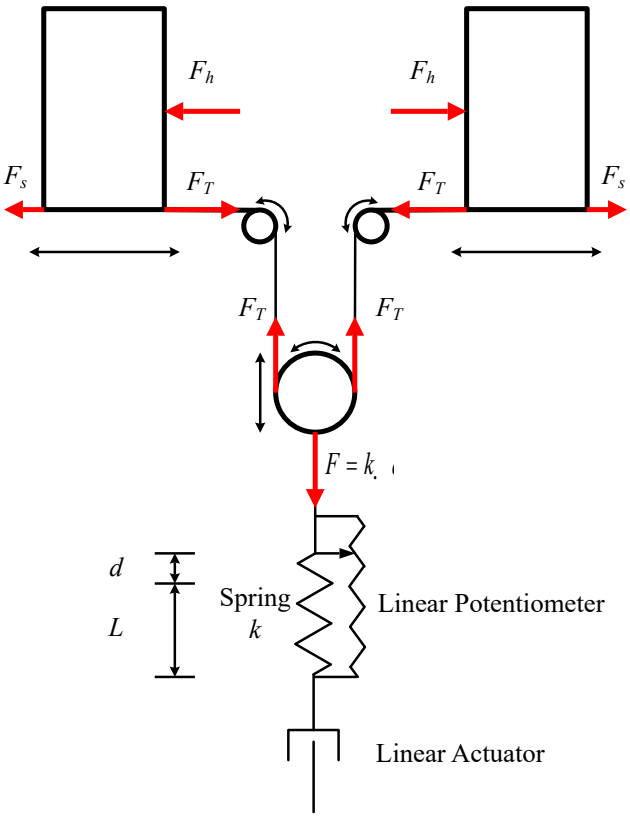

Figure 4.1: Line diagram depiction of the head stabilization device [23]

1. The mass of the foam head support blocks, sliders, cable, redirection and driving pulleys are negligible when compared to the weight of the head of an average person. As such, the inertial effects from these components may be neglected.

2. The sliding friction of head support blocks is small. Therefore, if one support block makes contact with the head before the other, as in the offset case, the contacting block will come to rest causing the free block to move twice as fast. The friction in the pulleys can also be neglected. The free rotation of the driving pulley also ensures that the cables leave the driving pulley at a 90° angle of departure.

3. The retraction force exerted by the constant force spring is assumed constant throughout the range of motion of the support blocks.

4. The spring constant of the extension spring is assumed constant throughout the range of operation of the subsystem.

It can be inferred through Fig. 4.1 that through control of the position of the linear actuator, the force applied to the head of the person can be controlled through variation of the position of the end effector, and thus can be controlled through the application of voltage to the motor. Thorough electromechanical modeling is presented later in the thesis. In the early experimentation, a PID controller with force feedback was implemented to achieve the desired system behavior. The feedback is measured by recording the deflection of the spring placed mechanically in series with the linear actuator, then calculating the applied force. With this feedback path, the feedback law can be written as follows:

$$\begin{aligned} f_{din}(t) &= 2(f_{dh}(t) + f_c) \\ e(t) &= f_{in}(t) - f_{din}(t) \\ \dot{e}(t) &= \dot{f}_{din}(t) \\ V_a(t) &= k_p e(t) + k_i \int e(t)dt + k_d \dot{e}(t) \end{aligned} \tag{4.2}$$

where f_{din} represents the desired input force to the system exerted by the linear actuator, f_{dh} represents the desired force applied to the head, f_c denotes the constant force applied by the retraction springs, f_{in} is the actual input force exerted by the linear actuator, V_a is the

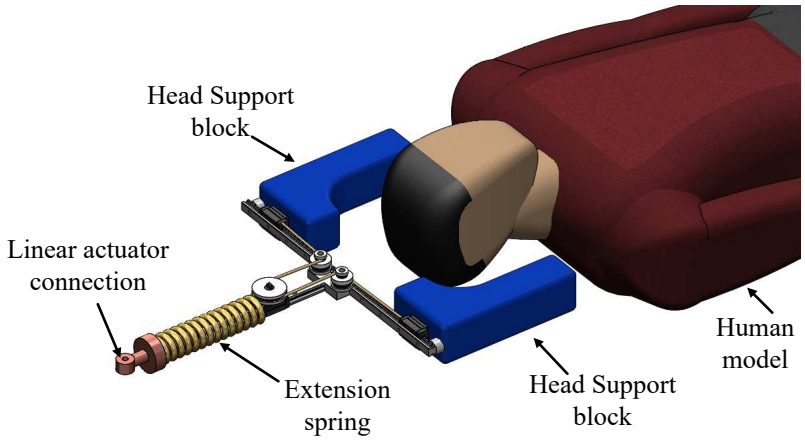

Figure 4.2: MSC ADAMS model of head stabilization device [23]

actuator voltage input as supplied through pulse width modulation (PWM), and k_p, k_i and k_d are the proportional, integral, and derivative gains, respectively.

4.2 Simulation of Force Control

Prior to applying the controller to the physical system, the validity of the proposed control scheme was tested using an MSC ADAMS-Matlab co-simulation. A co-simulation is one in which different parts of a system are modelled in separate software. Continuous exchange of information between the software during the simulation allows for the modelling of the complete system.

The physical head support system was completely modelled in ADAMS, with mass and inertia values corresponding to those of the actual system components. The input to the ADAMS model was the velocity output of the linear actuator, applied to the spring. The

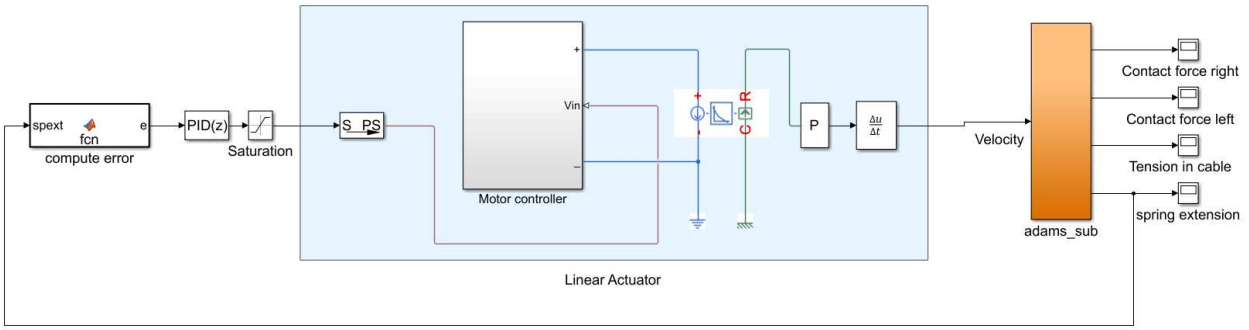

Figure 4.3: Simulink - MSC ADAMS Co-simulation Diagram [23]

model outputs were the extension of the spring (utilized as a feedback for the control algorithm), the force exerted by the blocks on the person's head, and the cable tension. The ADAMS model was then exported to Matlab as a Simulink block. Figure 4.2 shows the device as modeled in MSC ADAMS.

The linear actuator itself was modelled in Simulink using the Simscape-Electronic libraries. The generic linear actuator block in Simscape models the linear actuator based on force-speed characteristics of the actuator, efficiency of motor and estimated force-independent electrical losses all of which can be obtained from the datasheet of the actuator used [124].

Based on the spring displacement feedback from ADAMS, the force applied on the driving pulley is estimated. The PID controller then computes the voltage to be applied on the linear actuator based on the error. In order to model actuator voltage limits, a 12 V saturation block was applied to the output of the PID controller. The controller was then tuned for the proportional, integral and derivative gains resulting in the desired operation behavior. The constant retraction force, fc, was taken to be 1.07 N based on the retraction springs used in

the prototype. Thus, to reach the desired head support force, f_{dh}, of 10.0 N we can calculate the desired input force, f_{din}, to be 22.14 N based on Eq. 4.2. The overall block diagram of the co-simulation setup is shown in Fig. 4.3.

Figure 4.4 shows the simulation results with plots of desired head support force, f_{dh}, head support force applied, f_h, desired input force, f_{din}, and input force applied, f_{in}. The retraction springs apply an initial tension on the cable system, which causes f_{in} to jump by $2f_c$ early in the simulation. The head support blocks and the human were modeled as rigid bodies in ADAMS, resulting in an impact when they make contact with each other. The head support blocks make contact with the head at exactly 2 seconds, which causes a sudden spike in the f_h due to the impact. However, the spike does not occur in f_{in} values as the spring reduces the impulse during its extension. In the real system, the head support blocks are made of deformable foam that prevent an impact when they make contact with the injured person's head. The control system drives the linear actuator until f_{in} equals f_{din}, at which point f_h matches with f_{dh}. Together the two blocks will apply a total of 20 N support force on the head, which meets the design requirements. In result, the simulation shows that with proper tuning of the control gains the system is able to achieve the desired performance characteristics with a settling time below 5 seconds and steady state error within 0.1 N.

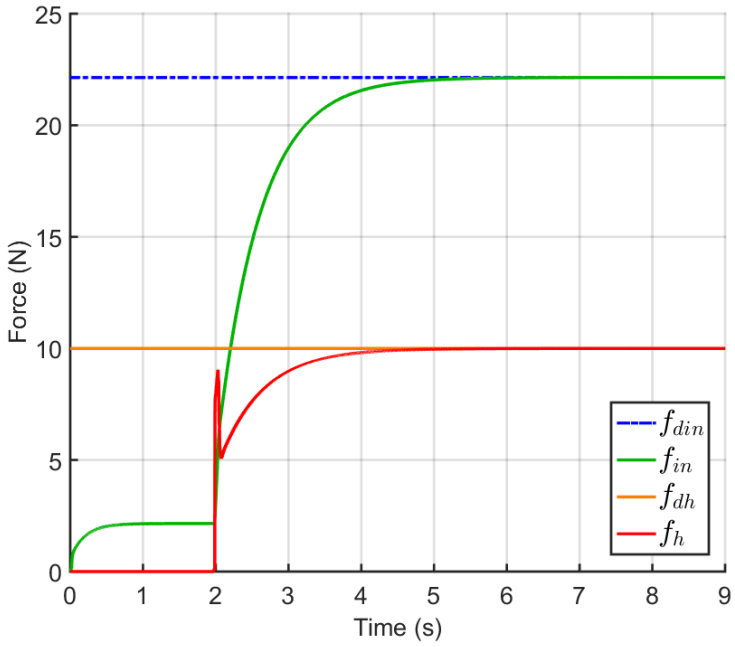

Figure 4.4: Results of force control co-simulation [23]

4.3 Proof-of-Concept Device for Control Testing

Based on the design goals and results of the simulation, a proof-of-concept prototype was fabricated to test the validity of the controller. Medical-grade foam head immobilization blocks from Morrison Medical were attached to rail-mounted sliding carts. The central pulley was also mounted atop a slider with a tempered steel extension spring (k = 478.1 N/m) fixed to the slider. The free end of the extension spring was then attached to a Firgelli LP16 linear actuator, creating a series elastic actuator. The linear actuator provided the draw force to the central pulley, which was then distributed to the head stabilization blocks through the differential mechanism. The controller was implemented on a Teensy 3.6 microcontroller, which outputs a PWM voltage signal to an H-bridge fed by a 12 VDC power

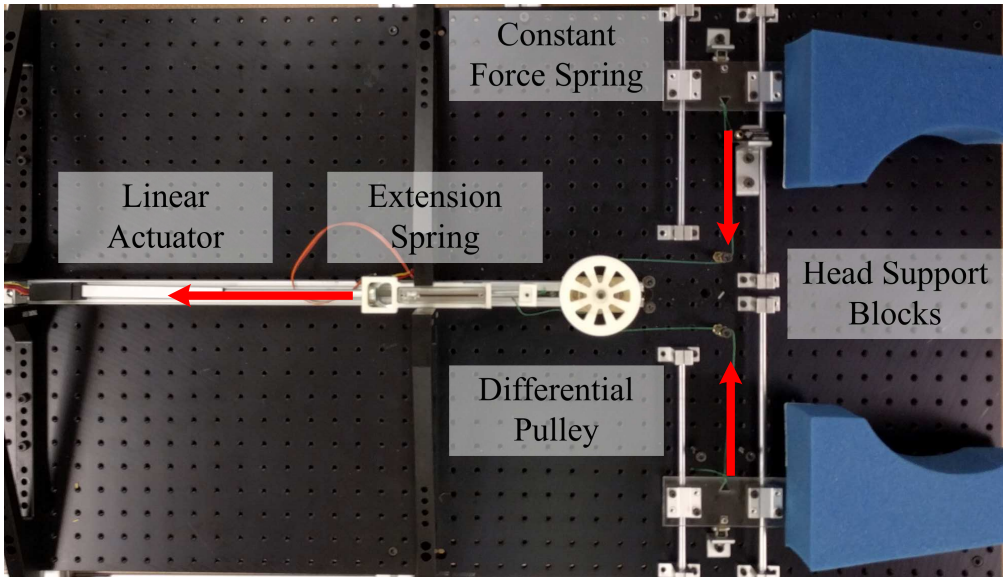

Figure 4.5: Proof-of-concept device used to test system force control [23]

source. In order to provide feedback of the input force, a linear potentiometer was mounted in parallel with the extension spring, which measured the spring deflection. Constant force springs providing 1.07 N restoring force was attached to the head blocks in order to return them to home position once the input actuation is removed. To validate the force relation between the force applied on the head, f_h, and the input force, f_in, a Transducer Techniques MLP-10 single axis load cell was positioned to provide a mechanical stop for the rigid base of the head support blocks. The output signal was conditioned by a TMO-2 +/- 10VDC signal conditioner. A more sophisticated method to measure the force applied directly by foam head support blocks will be the subject of future work. An image of the proof-of-concept prototype may be found in Fig. 4.5.

To validate the control system on a physical prototype, the controller was set at a desired

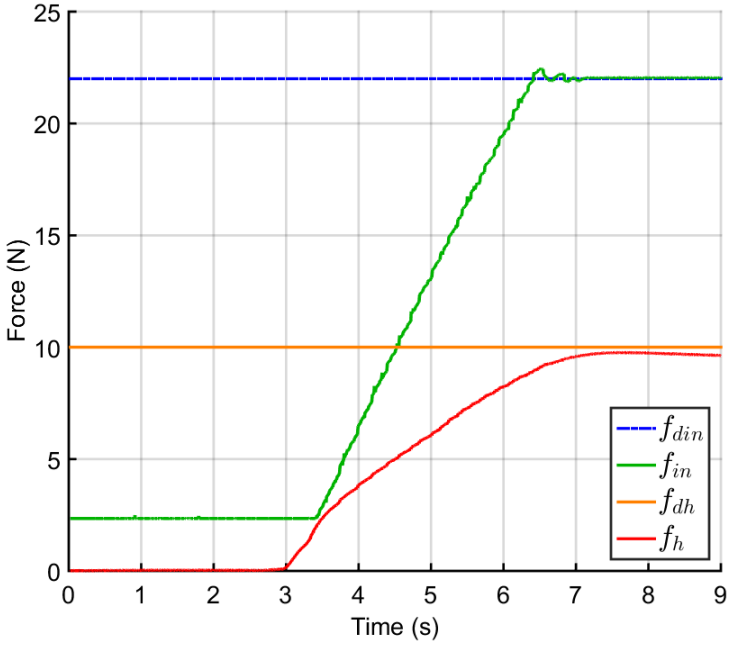

Figure 4.6: Experimental results of control test with proof-of-concept system [23]

input force f_{din}, to be 22.14 N based on the same calculations as for the simulation. The data was collected form the linear potentiometer and the single axis load cell. The data from the linear potentiometer was used to estimate the total input force to the system at the SEA, f_{in}. The force applied by one head block was directly measured by the load cell. The results can be seen in Fig. 4.6.

The results show very similar behavior to that of the simulation. The measured f_in, estimated from the extension of the spring starts from approximately 2N due to the tension generated by the retraction springs, which is equal to $2f_c$. During the experiment, the head support blocks make contact at about 3 seconds, which causes an increase in f_in starting at 3.5 seconds. The control system then drives f_in almost linearly to the desired value of 22.14

N.

The force measured by the load cell, corresponding to the force applied to the head, f_h, varies more from the simulation. The simulated head force shows an impulse due to contact, followed by a short mechanical settling period where the controller continues to apply force. In the experimental results, the measured head force shows no impulse as well as a slight decay in the steady state value. Both behaviors are due to characteristics of load cells and the signal filtration applied to remove high frequency noise. In all, results show that the physical system was able to meet the desired requirements with a settling time less than 8 seconds.

Chapter 5

Design, Control, and Experimentation with Updated Prototype

5.1 Electro-Mechanical Design

In redesigning the head stabilization subsystem, there were several key goals to be met in order to ensure the proper operation. The primary goal is that force be applied equally at the application points in order to reduce discomfort and provide a secure and stable hold when restricting the motion of the head. Additionally, the device must be able to hold the head stable in the presence of outside disturbance, such as vibration during transport on an ambulance or autonomous robot. Finally, the subsystem must be lightweight and low profile to facilitate easy transport, while also reusable and easily sterilized.

However, the experimentation showed that the incorporation of the linear actuator and the sliding differential pulley was both too slow and too large for practical implementation. Thus it was determined that future designs required a rotary motor as well as a more compressed form factor in order to provide a workable design. Furthermore, while the PID controller implemented in [23] performed well, a more effective feedback controller for rejection of disturbances was desired. This objective is addressed in Section 4.

With the above goals as the guiding influence, the resultant mechanical design of the head stabilization device can be seen in Fig. 5.1. Two shaped medical grade foam head blocks act to provide compliant support in direct contact with the head of the injured person. A rigid frame forms a low-profile structure to support the mechanical components as well as holding the fabric base piece upon which the head rests during stabilization. The treated nylon fabric base is held taut between the arms of frame, and can both be easily disinfected or replaced as needed. The use of fabric for the head rest location allows the device to be slid under a person's head with minimum clearance, and provides a measure of compliance while supporting the head. A plastic cover protects the motor and moving parts as well as helps to prevent headwear or hair from becoming caught in the mechanism.

The two head support blocks are mounted on thin aluminum plates, which are then rigidly fixed to sliding carts. The carts are actuated via a cabling system, which allows for compliant motion of the blocks. Defined by Hirose in [106], a compliant mechanism redistributes the dynamic inputs of a system mechanism are balanced between multiple degrees of freedom (DOF). The design thus apportions the applied forces equally between the each foam piece,

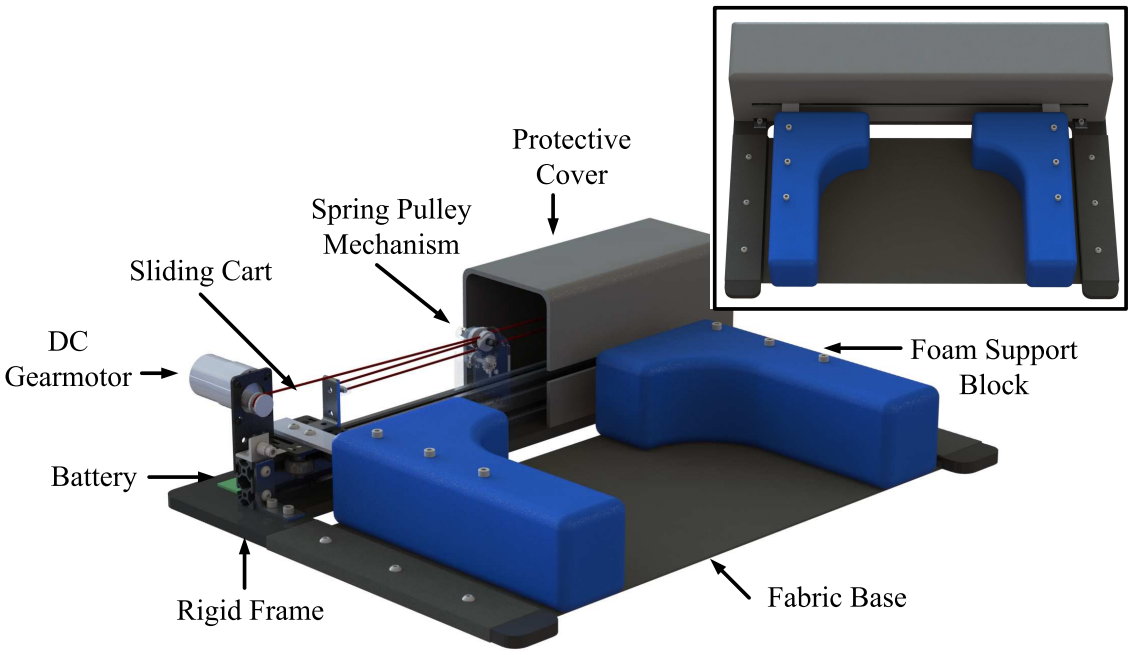

Figure 5.1: Updated subsystem design [24]

and allows the two to support the head in asymmetrical configurations. This action is key in providing a stable support without placing undue force upon the head and neck on an injured person, particularly when implemented by an autonomous rescue robot. While trained medical professionals have the skills to analyze an injury and determine whether re-aligning the cervical spine is safe, an autonomous robotic system is much better served in stabilizing *in situ* as best as possible and waiting until human medical attention is available.

The cabling system that drives the motion of the two blocks is depicted in Fig. 5.2. The cable is driven using an electric motor, and two constant force springs are included to provide a constant retraction force such that when the motor feeds more cable into the system, the blocks move away from eatch other. The motor pulley, M, rotates and acts to pull the two

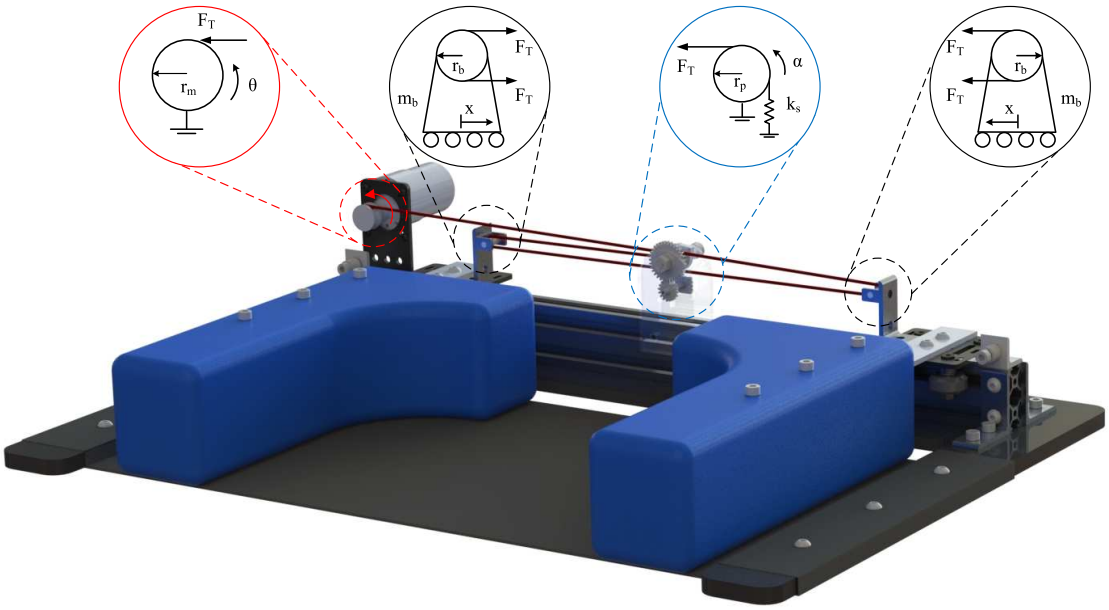

Figure 5.2: Cabling details and free body diagrams for relevant components [24]

blocks mounted upon the sliding carts together by reducing the total length of the cable. The spring pulley is held fixed by a spring grounded at the opposite end, with a spring constant k_s. Until an external force is applied to the system, the spring pulley acts as a fixed cable termination (assuming the sliding carts' motion is frictionless). If one cart makes contact, the second cart accelerates to travel at a multiple of the original speed inversely proportional to the until contact is made with both foam support blocks due to the nature of the cabling. This is shown by differentiating the total length of the cable and relating this to the change in position of the supporting block, $\dot{x}$, such that $\dot{\Theta} = \frac{2}{r_m}\dot{x}$. Once bilateral contact is initiated, the compliance of the mechanism acts to distribute the force equally between the two sides.

Once force is applied to the head by the two blocks, the spring pulley rotates with a corre-

sponding linear displacement equal to $\delta_c = \alpha r_p$, where δ_c is the change in cable length, α is the angular displacement, and r_p is the radius of the pulley. The torsional spring then exerts a force equal to $F = \delta_c k_s$. Therefore, by measuring the rotation α of the pulley, the applied force can be mapped and thus utilized as the feedback for the controller. The overall subsystem can be envisioned as a variant of a series elastic actuator [122].

Biomechanical studies performed in [123] were utilized to determine the required stabilization force to be provided by the subsystem. Research shows that the muscles that anchor the head and cervical spine exert a force of approximately 16 N perpendicular to the spine to provide roughly 35 degrees of rotation. Therefore, to adequately restrict unwanted motion initiated by the patient and environment, the desired force applied by the subsystem is a net 20 N, with the force applied by each support block, F_h, equal to 10 N .

The effect of friction in the pulley system was taken into consideration while considering the model of the force applied to the head by the support blocks. The standard pulley friction model is given by $F_{T,1} = F_{T,2} \exp \mu\gamma$, where μ is the coefficient of static friction between the pulley and cable, γ is the cable wrap angle and $F_{T,1}$ and $F_{T,2}$ are the tension forces

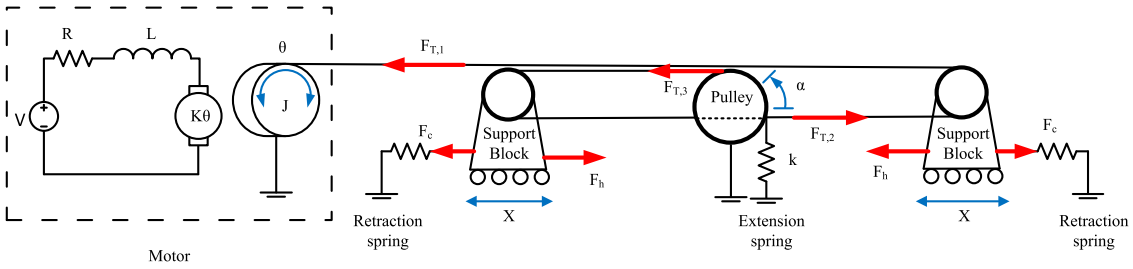

Figure 5.3: Electromechanical model of the head stabilization device [24]

on either side of the pulley. Based on the arrangement of the system as described in Fig. 5.2, the wrap angle for both sliding block pulleys is less than $\pi/2$ radians due to the motor and spring spool pulleys being larger than in diameter than the redirection pulleys. The coefficient of friction for the ultra-high-molecular-weight polyethylene cable utilized in the system running on a metal pulley is less than 0.1. Thus for the above specifications, $\exp \mu\gamma$ approached unity, rendering the effect of friction on the system negligible and the frictional forces can be considered equal to F_T. This the results in the necessary tension force in the cable, F_T, being half of the force applied to the head once bilateral contact is made, such that $F_T = \frac{F_h + F_c}{2}$. Additionally, the tension force at the spring pulley is directly proportional to the rotation of the spring pulley due to the spring, resulting in $F_T = \alpha r_p k_s$. Combining these two equations, along with the relation between the spring pulley and motor pulley rotation, $\alpha = \theta r_m$ results in the direct coupling between force and motor rotation, $F_T = \theta r_m r_p k_s$. A set of free body diagrams depicting the forces applied to the motor, support blocks, and spring pulley are shown in Fig. 5.2, with an illustration of the translation of forces in Fig. 5.3.

The device can be modeled as an electro-mechanical system through the electrical and mechanical models for DC motors given below.

$$\begin{aligned} V(t) &= R_a i_a(t) + L_a \frac{di_a}{dt}(t) + nK_E \Theta_m(t) \\ T_l(t) &= J\ddot{\Theta}(t) + B\dot{\Theta}(t) + T_s \\ T_l(t) &= nK_T i_a(t) \end{aligned} \tag{5.1}$$

where V represents the armature voltage applied to the motor, R_a is the armature resistance, L_a denotes the armature inductance, i_a is the armature current, n represents the gear ratio, K_E is the electromotive force constant, and Θ_m denotes rotor position. The rotor position is equal to the motor pulley position multiplied by the gear ratio n, $\Theta_m = n\Theta$. Additionally, the load torque is represented by T_l while J denotes the combined motor and gearbox inertia, and B is the motor and gearbox damping. The torque contributed by the spring displacement is $T_s = \Theta_m r_p k_s$. Finally, the load torque is related to the armature current by the motor torque constant K_T. Using the three electromechanical motor equations and the relation between tension force and motor rotation, the resultant system transfer function is shown below in Eq. 5.2

$$\frac{F_T}{V} = \frac{2nK_T r_m r_p k_s}{JL_a s^3 + (JR_a + BL_a)s^2 + (R_a B + n^2 K_e K_t + L\frac{r_p k_s}{B})s + R\frac{r_p k_s}{B}} \tag{5.2}$$

It can be observed that the resultant system is a third order system due to the presence of the integration introduced when relating motor torque to angular position. The time constants of the electrical and mechanical systems are represented by $\tau_e = \frac{L_a}{R_a}$ and $\tau_m = \frac{J_m}{B_m}$. As the electrical time constant is negligible relative to the mechanical time constant, its effects on the dynamic system can be ignored, thus resulting in the reduced order model in Eq. 5.3

$$\frac{F_T}{V} = \frac{2nK_1 r_m r_p k_s}{\tau_m s^2 + (K_2 + 1)s + K_3} \tag{5.3}$$

where $K_1 = \frac{nK_t}{R_a B_l}$, $K_2 = \frac{n^2 K_t K_e}{R_a B_l}$, and $K_3 = \frac{r_p k_s}{B_l}$. The reduced order model simplifies the

control of the system and helps to guarantee the stability of the controller introduced in the following section.

5.2 Controller Design

Ultimately, the goal in providing support of the head and neck of an injured person is to minimize any undue angular oscillations of the head with respect to the neck. This prevents further damage to the possibly damaged vertebrae. To this end, it is ideal that the controller maintaining the securing force on the head would act to reject outside oscillatory or impulsive disturbances that may be injected into the system. Possible sources of such disturbances include vibrations from rough terrain being traversed by a rescue robot, or vehicle dynamics imposed by robot locomotion modules or transport in an ambulance.

While model-based controllers are often used in such situations, the system as designed provides difficulties in accurately estimating a variety of model properties. The compliance of the foam support blocks introduces variable damping as well as spring elements that are difficult to ascertain, and may vary with compression. Furthermore, the effective mass in the system is provided by the head being stabilized, which will be different for each person being stabilized and is also dependent on factors such as headwear. Additionally, a conscious person with some degree of muscle control will require a lesser degree of stabilization than an unconscious patient, whose head will freely move in response to stimulus.

In pursuit of such a feedback controller, active disturbance rejection control (ADRC) is imple-

mented for the system. Fully articulated by Han in [125], the controller is at the intersection between classic PID control and modern model-based control theory. The key aspect is that the entire system, including external disturbances, is captured utilizing an extended state observer (ESO). Once so estimated, the disturbances can be compensated for, all without requiring any model specific knowledge of the system beyond assumption of a base canonical state space formulation. While the seminal work on ADRC features a nonlinear state estimator and control law, the system presented here utilizes a linearized version (LADRC) [126, 127]. In LADRC, the nonlinear estimator is replaced with a Luenberger observer and coupled with a proportional-derivative controller.

As shown above,the head stabilization device can be represented as a second-order, single-input-single-output system, whose plant can be represented by $\ddot{y} + a\dot{y} + by = bu + w$. In this representation, a and b are unknown as they cannot be accurately modeled due to the presence of frictional effects and the compliance of the foam support blocks.However, some knowledge is present of the system, such that b_0 can be estimated such that $b = b_0 + b_{err}$. Further, while u is the known control input, w is the unknown external disturbance, which includes signal noise, external impulses, and model estimation error, b_{err}.

In the LADRC scheme diagrammed in Fig. 5.4, the state vector, x, contains the first and second order response of the system, x_1 and x_2, as well as a third, augmented state, $x_3 = f(y, \dot{y}, u, w)$, that encapsulates the plant's behavior, inclusive of the external disturbance. Incorporating f into the plant enables the reduction of the second order system to the form shown in Eq. 5.4

$$\ddot{y} = f + b_0 u \tag{5.4}$$

If an estimation of f is determined, the estimation, $\hat{f}$, can be incorporated into the two step PD control law found in Eq. 5.5.

$$\begin{aligned} u_0 &= k_p(r - \hat{x}_1) - k_p \hat{x}_2 \\ u &= \frac{-\hat{x}_3 + u_0}{b_0} \end{aligned} \tag{5.5}$$

Substituting into Eq. 5.4, it can be seen that the control law is structured such that the system can be reduced to a unit gain double integrator control system [126]:

$$\ddot{y} = (f - \hat{f}) + u_0 \tag{5.6}$$

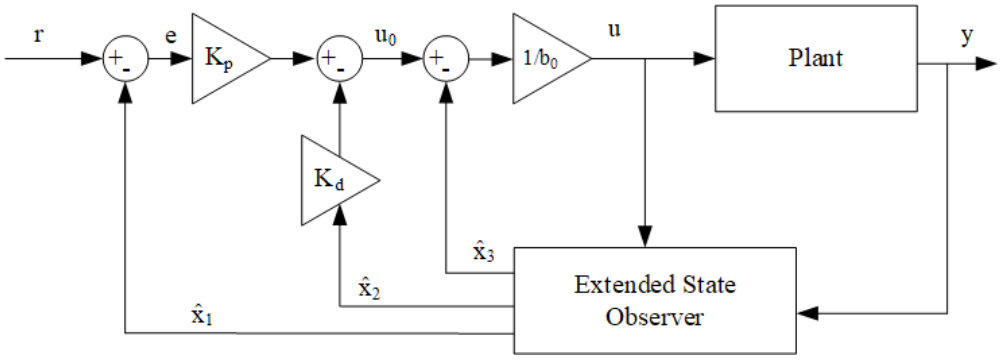

Figure 5.4: System control block diagram

In state space, this system is represented as Eq. 5.7:

$$\begin{cases} \dot{x}_1 = x_2 \\ \dot{x}_2 = x_3 + b_0 u \\ \dot{x}_3 = \dot{f}(y, \dot{y}, u, w) \\ y = x_1 \end{cases} \tag{5.7}$$

The system can then be estimated through the implementation of a Luenberger observer in Eq. 5.8

$$\begin{aligned} \dot{\hat{x}} &= A\hat{x} + Bu + L(y - \hat{y}) \\ y &= C\hat{x} \end{aligned} \tag{5.8}$$

where

$$A = \begin{bmatrix} 0 & 1 & 0 \\ 0 & 0 & 1 \\ 0 & 0 & 0 \end{bmatrix}, B = \begin{bmatrix} 0 \\ b_0 \\ 0 \end{bmatrix} C = \begin{bmatrix} 1 \\ 0 \\ 0 \end{bmatrix} L = \begin{bmatrix} \beta_0 \\ \beta_1 \\ \beta_2 \end{bmatrix}$$

Through parametrization of the controller and observer gains [126], stable gains are chosen for the control system. As Eq. 5.6 can be approximated as the second order system $\ddot{y} \approx u_0$ given the accuracy of the estimated disturbance, the control gains are chosen as $K_p = 2\zeta\omega_c$ and $K_d = \omega_c^2$, where ω_c and ζ are the desired closed loop natural frequency and damping, respectively.Further, these gains are chosen such that they correspond to real valued negative poles for the closed loop system, ensuring the stability of the PD controller.

When considering the Luenberger observer, the error dynamics of the estimated system are

determined by the resultant matrix of (A-LC):

$$A - LC = \begin{bmatrix} \beta_0 & 1 & 0 \\ \beta_1 & 0 & 1 \\ \beta_2 & 0 & 0 \end{bmatrix} \tag{5.9}$$

To guarantee the stability of the observer, the roots of $\lambda_o(s) = s^3 + \beta_0 s^2 + \beta_1 s + \beta_2$ must be in the left hand plane. For simplicity, the three poles can be placed at a common point, ω_o, representing the bandwidth of the observer. Equivalently, $\lambda_o(s) = (s + \omega_o)^3$ and thus $\beta_0 = 3\omega_o$, $\beta_1 = 3\omega_o^2$ and, $\beta_2 = \omega_o^3$

In order to effectively implement LADRC on a microcontroller, the observer was discretized using zero-order hold (ZOH) [127]. Following discretization, the observer would be considered to be in the form of a "predictive discrete observer" of shown in Eq. 5.10:

$$\dot{\hat{x}}_{k+1} = A_d \hat{x}_k + B_d u_k + L(y_k - C_d \hat{x}_k) \tag{5.10}$$

where the subscript d represents the discretized version of a matrix. It can thus be understood that the predictive observer utilizes current state and system feedback to predict the future states of the system. However, low-sampling rates or communications delays may introduce error in the predictions and thus instability in the controller. As a method of proofing the observer against such instabilities, it can be configured as a "current observer" [128], resulting in the discrete observer seen in Eq. 5.11

$$\hat{x}_k = A_{co}\hat{x}_{k-1} - B_{co}u_{k-1} + Ly_k \tag{5.11}$$

where

$$A_{co} = A_d - LC_dA_d$$

$$B_{co} = B_d - LC_dB_d$$

The discretized control law is represented by Eq. 5.12

$$\begin{aligned} u_{0,k} &= K_p(r_k - \hat{x}_{1,k}) - K_d\hat{x}_{2,k} \\ u_k &= \frac{-\hat{x}_{3,k} - u_{0,k}}{b_0} \end{aligned} \tag{5.12}$$

While the PID gains are unchanged following the discretization of the system, the observer error dynamics vary, resulting in an updated observer gain matrix as determined by the discretized coefficient matrices and the desired observer natural frequency ω_o, discretized such that $\beta = e^{-\omega_o T_s}$.

$$Lc = \begin{bmatrix} 1-\beta^2 \\ (1-\beta)^2(1+\beta)\frac{3}{2T_s} \\ (1-\beta)^2\frac{1}{T_s^2} \end{bmatrix} \tag{5.13}$$

5.3 System Simulation

In order to test and compare the proposed control methodologies, the system pictured in Fig. 5.4 was simulated as a discrete time model in MATLAB. The plant of the system was modeled

as a canonical second-order system of the form $G(s) = \frac{{\omega_n}^2}{s^2+2\zeta\omega_n s+{\omega_n}^2}$. The system properties were estimated through the application of Nelder-Mead simplex optimization through the MATLAB `fminsearch` function, fitting the model to data collected when testing the proof-of-concept prototype in [22].

As a reference case, the simulation was tested both with a PID controller in addition to with the LARDC controller. The first task was to verify the controllers' response to a step input of 10 N occurring at 0.2 s, to verify that LARDC performs as well as the PID in absence of disturbance. In both cases, the controller outputs were passed through a saturation limit at the motor's top speed. The two controllers can be seen to have almost identical rise times, and less than 10% overshoot. The results of this simulation are found in Fig. 5.5

Following the validation of the control behavior in an undisturbed system, the controllers were tested with both a momentary step disturbance of 5 N at 0.25 s, held for 0.1 s as well as with a sinusoidal disturbance with an amplitude of 5 N and a frequency of 30 Hz. While PID rejects the majority of the disturbance, with roughly a 1% deviation from the setpoint, the LADRC model demonstrates almost no disturbance at all. The disturbance rejection abilities of LADRC are demonstrated when a sinusoidal disturbance is injected into

	PID	LADRC
Step Disturbance	15.3385	0.1922
Sinusoidal Disturbance	72.973	1.6603

Table 5.1: Sum of L_1 Norms of Error for Controllers

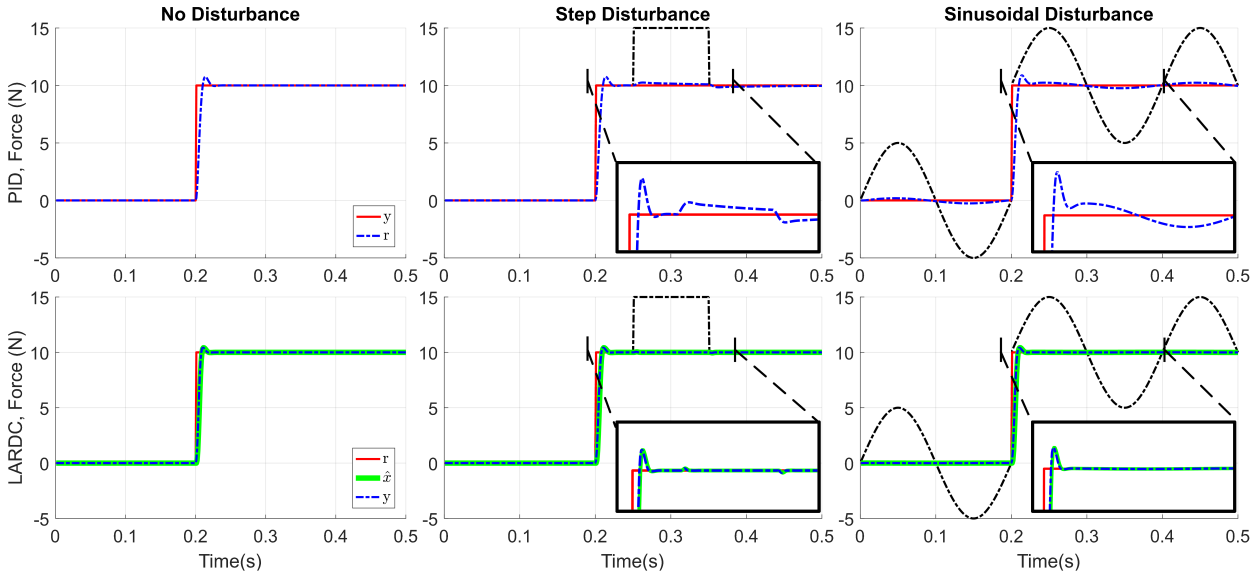

Figure 5.5: Controller comparison with a step input for no disturbance, a step disturbance, and a sinusoidal disturbance, with insets highlighting the respective disturbance rejection abilities [24]

the system as well.

The sum of the L_1 norms of the error with relation to the setpoint for the PID and LADRC controllers are shown in Table 5.1. The error values are corrected for the initial controller tracking by subtracting the error incurred with no disturbance.

In the case of a step disturbance, LADRC provides almost complete rejection of the unwanted input. The PID controller, while tuned to have a nearly identical rise time as the LADRC, demonstrates good rejection behavior as well, but requires a non-trivial amount of time to recover completely from the disturbance. This improved steady state error minimization in the LARDC implementation derives from the removal of steady state error through the

observed augmented state, rather than the necessity of including an integral term.

When the system is injected with a sinusoidal disturbance, LADRC again demonstrates superior performance removing the effects of the injected disturbance signal, with a nearly sevenfold reduction in integral error over the duration of the simulation. This type of disturbance in more in line with the higher frequencies encountered when a vehicle travels over rough terrain.

The simulation results show that LADRC offers improved disturbance rejection behavior, without the necessity of including an integrator to the system. The superior operation justifies the use of LADRC when building a physical prototype of the system for experimentation.

5.4 Experimental Validation

In order to validate the performance of the system, a physical prototype was fabricated and experiments were conducted. For the rigid base, an acrylic frame was manufactured. A brushed DC gearmotor is the central actuator for the system, with a no load speed of 200 RPM and a stall torque of 1.2 N-m. The control system is implemented on the prototype utilizing an ARM Cortex-M4 microcontroller with a clock speed of 96MHz. The prototype can be seen in Fig. 5.6

In order to provide a simulacrum for a human head, a weighted, to-scale foam model was utilized when conducting experiments. A 3-axis joystick was affixed to the neck in order to provide feedback on the roll, pitch and yaw of the head relative to the neck during

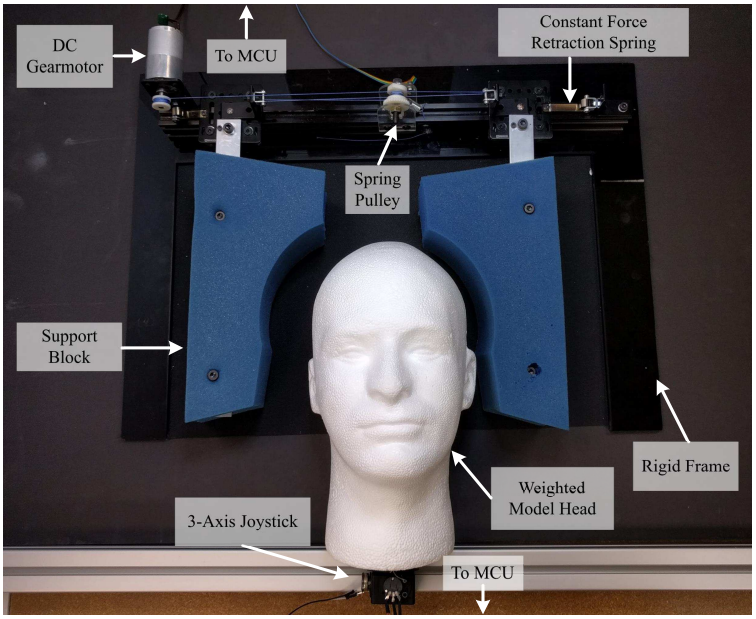

Figure 5.6: Head stabilization device prototype [24]

stabilization, providing angular feedback with a maximum range of ±54°. A second ARM Cortex-M4 microcontroller ran concurrently in order to collect the angular data.

In the first experiment, the head stabilization device received a step input of 10 N. The estimated state feedback, the system feedback, the setpoint, and the Euler angles of the head model were simultaneously recorded. The results are shown in Fig. 5.7. The controller exhibits critically damped behavior, desirable to minimize any impulses incurred when contact with the patient head. The extended state observer shows excellent tracking behavior, with very little estimation error. Despite the application of significant force by the support blocks, the head shows minimal angular displacement. The roll, pitch and yaw angles had maximums of 3.1°, 1.3°, and 2.5° respectively. The stepwise behavior of the system as force is applied is due to the gearing utilized to translate the rotation of the central shaft to the

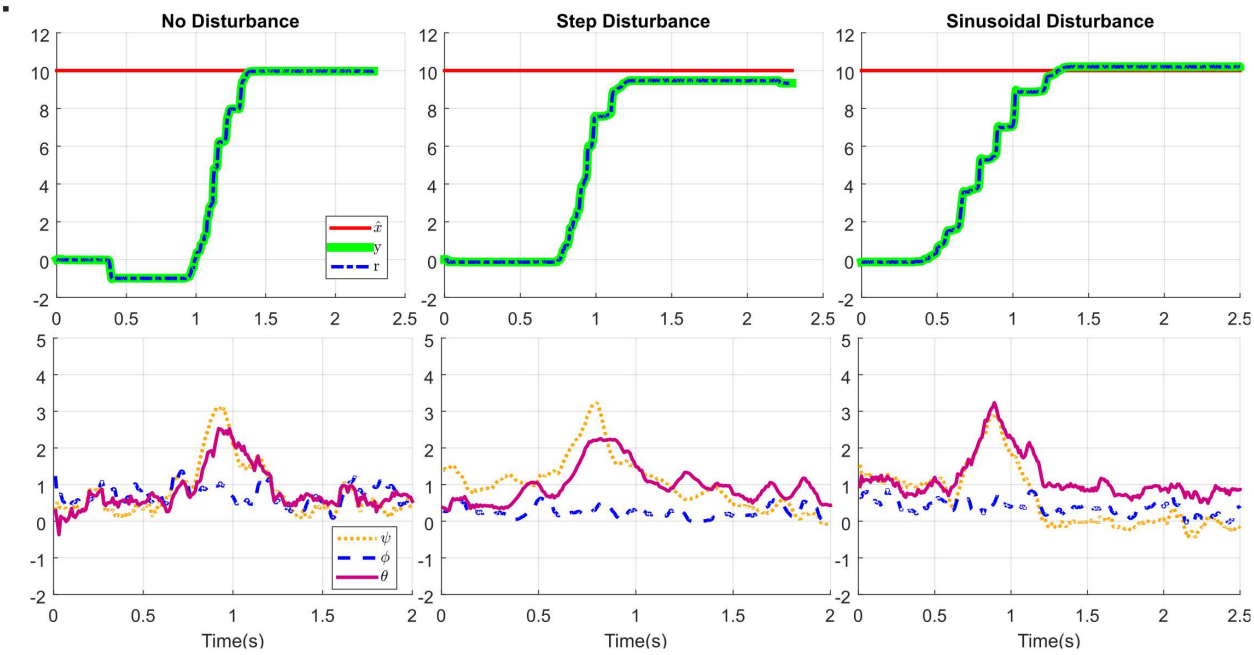

Figure 5.7: Experimental angular and force feedback results from system with no disturbance, a step disturbance, and a sinusoidal disturbance

potentiometer. Future implementations of the system will seek to avoid this through the use of a belt drive or direct measurement.

The disturbances seen by the system in the act of stabilizing the head of a rescued person during transport can be broadly categorized into three main modes. The first such disturbance would be due to the presence of a momentary unilateral force disturbance, e.g. caused by the motion of the prone person's entire body, possibly due to centripetal force during a turn. In this case, the desired behavior is to allow the translation of the body, neck, and head so as not to cause undue shear forces in the neck and possibly exacerbate any injuries. This disturbance mode is compensated for by the differential mechanism. In response to unilateral force, the entire block-head-block system will translate laterally in response to

the disturbance, while maintaining force upon the head, due to the translation of the cable through the pulley system.

The second type of disturbance the system would encounter is a constant bidirectional force disturbance applied to each support block equally caused by a roll-inducing moment in the head, e.g. a conscious person turning their head. In such a case, the control system acts to maintain the commanded reference force, and in response to the increased force feedback would act to reduce the applied force at the support blocks.

Finally, the third disturbance mode is due to low frequency oscillatory force induced by the motion of the platform upon which the person and head stabilization device, such as caused by the vibration of a vehicle on rough terrain. This disturbance mode contains elements of the other two, in that the oscillations can both cause full-body translations and induce head roll. In addition, out of phase oscillatory motion between the head and the body which may

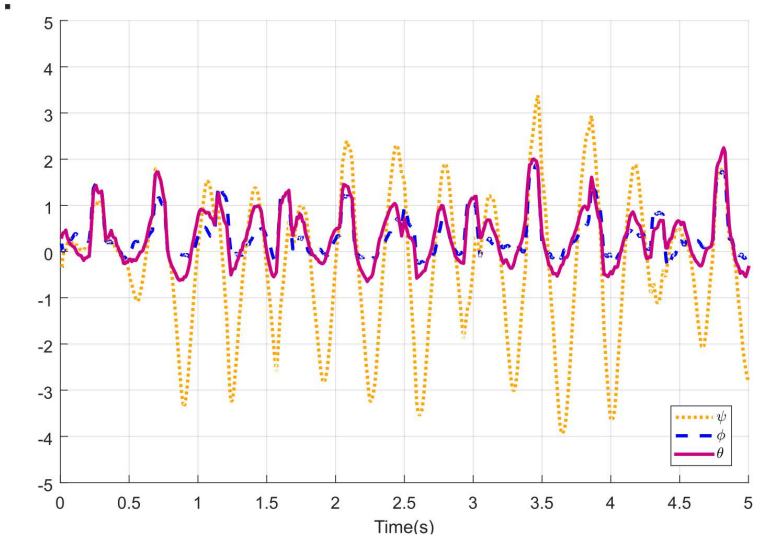

Figure 5.8: Effect of Type 3 disturbance on the head model with no stabilization

be deleterious to the health of the patient. In such a case, the control system will act to reduce the force disturbances while maintaining the reference force, which in turn also acts to reduce the asynchronous oscillations between the head and body.

To validate the rejection of a Type 3 disturbance by the system, the entire platform upon which the head stabilization unit, the head model, and the angular measurement device were placed was injected with a sinusoidal input with a frequency of approximately 5 Hz. The effect on the angular displacement of the unsupported head can be seen in Fig. 5.8. The disturbance was then repeated as the system attempted to stabilize the model head while data was recorded.

The results of this experiment are shown in the third column of Fig. 5.7. The disturbance rejection properties of the controller are again demonstrated, as the force disturbances are nearly fully minimized and the angular disturbances beyond the those due to the initial impact were nearly completely reduced.

In summary, the experiments validate the performance of the system and establish its ability to stabilize the head and neck of an injured person during medical transport. When presented with both step and sinusoidal disturbances, the experimental results replicate the results predicted in the simulation of the control system, and show that LADRC is an effective control system for the rejection of disturbances.

Chapter 6

Conclusion & Future Work

This chapter concludes the thesis, as well as provides a short description of the future work to be implemented on the head stabilization device and SAVER overall.

6.1 Conclusion

This thesis introduces a comprehensive review of the field-deployed search and rescue robots to date. The design and control of a head stabilization device are presented, along with the prototype construction and experimental testing. A differential mechanism was integrated into the design in order to enable a compliant and balanced force control environment. While PID force control was initially tested, in order to provide improved immunity to outside perturbations linear active disturbance rejection control (LADRC) was implemented both in simulation and experiment. The design and control exhibited excellent force control and

disturbance rejection behavior, and successfully met the desired design goals.

6.2 Future Work

Future plans for the head stabilization device will couple with the shoulder gripping arms in order to fully test the retraction unit. Following integration of the two subsystems, the declining stretcher will be prototyped to provide a full retraction trial, utilizing an artificial human model to provide demonstration of the feasibility of the system. The ultimate goal is to build and bench test each critical subsystem of SAVER, eventually composing a completed platform of fully tested subsystems that can be demonstrated in comprehensive live tests that demonstrate the designed capabilities of the system.

Chapter 7

Bibliography

[1] R. R. Murphy, J. Kravitz, S. L. Stover, and R. Shoureshi, "Mobile robots in mine rescue and recovery," *IEEE Robotics and Automation Magazine*, vol. 16, no. 2, pp. 91–103, jun 2009. [Online]. Available: http://ieeexplore.ieee.org/document/5069840/

[2] S. Odedra, S. Prior, and M. Karamanoglu, "Investigating the Mobility of Unmanned Ground Vehicles," in *International Conference on Manufacturing and Engineering Systems. Proceedings*, no. January, 2009, pp. 380–385. [Online]. Available: http://eprints.mdx.ac.uk/3863/

[3] Human-Robot Informatics Laboratory, "Disaster Response Robot Quince," 2012. [Online]. Available: http://www.rm.is.tohoku.ac.jp/quince_eng/

[4] R. R. Murphy, S. Tadokoro, D. Nardi, A. Jacoff, P. Fiorini, H. Choset, and A. M. Erkmen, "Search and Rescue Robotics," in *Springer Handbook of Robotics*. Berlin,

Heidelberg: Springer Berlin Heidelberg, 2008, pp. 1151–1173. [Online]. Available: http://link.springer.com/10.1007/978-3-540-30301-5

[5] G.-J. M. Kruijff, F. Pirri, M. Gianni, P. Papadakis, M. Pizzoli, A. Sinha, V. Tretyakov, T. Linder, E. Pianese, S. Corrao, F. Priori, S. Febrini, and S. Angeletti, "Rescue robots at earthquake-hit Mirandola, Italy: A field report," in *2012 IEEE International Symposium on Safety, Security, and Rescue Robotics (SSRR)*, no. July. IEEE, nov 2012, pp. 1–8. [Online]. Available: http://ieeexplore.ieee.org/document/6523866/

[6] J. Casper and R. R. Murphy, "Human – Robot Interactions During the Robot-Assisted Urban Search and Rescue Response at the World Trade Center," *IEEE Transactions on Systems, Man and Cybernetics*, vol. 33, no. 3, pp. 367–385, 2003.

[7] A. Williams, B. Sebastian, and P. Ben-Tzvi, "Review and Analysis of Search, Extraction, Evacuation, and Medical Treatment Field Robots," *Journal of Intelligent and Robotic Systems*, p. Under Review, 2017.

[8] B. Yamauchi, "The Robot Gallery," 2005. [Online]. Available: http://robotfrontier.com/gallery.html

[9] A. C. Yoo, G. R. Gilbert, and T. J. Broderick, "Military Robotic Combat Casualty Extraction and Care," in *Surgical Robotics*. Boston, MA: Springer US, 2011, pp. 13–32. [Online]. Available: http://link.springer.com/10.1007/978-1-4419-1126-1_2

[10] G. R. Gilbert and M. K. Beebe, "United States Department of Defense Research in Robotic Unmanned Systems for Combat Casualty Care," NATO/RTO, Tech. Rep., 2010.

[11] Hstar Technologies, "HStar Technologies - cRoNA Combat Casualty Extraction and First Responder Robot," 2012. [Online]. Available: http://www.hstartech.com/index.php/crona.html

[12] Y. Iwano, K. Osuka, and H. Amano, "Posture manipulation for rescue activity via small traction robots," in *IEEE International Safety, Security and Rescue Rototics, Workshop, 2005.*, vol. 2005, no. June. IEEE, 2005, pp. 190–195. [Online]. Available: http://ieeexplore.ieee.org/document/1501262/

[13] ——, "Experimental study of traction robot system for rescue against nuclear disaster," in *IEEE International Safety, Security and Rescue Rototics, Workshop, 2005.*, vol. 2005, no. June. IEEE, 2005, pp. 222–227. [Online]. Available: http://ieeexplore.ieee.org/document/1501267/

[14] Lockheed Martin, "SMSS: The Right Solution at the Right Time," 2013. [Online]. Available: http://www.lockheedmartin.com/content/dam/lockheed/data/mfc/pc/smss/mfc-smss-pc.pdf

[15] Qinetiq, "Titan: Dismounted Troop Support System," Tech. Rep., 2016. [Online]. Available: https://www.qinetiq-na.com/wp-content/uploads/DataSheet_Titan_Nov2016.pdf

[16] HDT Global, "HDT Protector Robot," Tech. Rep., 2016. [Online]. Available: http://www.hdtglobal.com/wp-content/uploads/2015/01/HDT_Protector_Robot_26.pdf

[17] C. M. D. Hill, "The Role of Robotic Technology in a Manned Mission to Mars," 2015. [Online]. Available: https://www.asme.org/career-education/early-career-engineers/me-today/new-documentthe-role-robotic-technology-manned

[18] J. Rosen, M. Lum, M. Sinanan, and B. Hannaford, "Raven: Developing a Surgical Robot from a Concept to a Transatlantic Teleoperation Experiment," in *Surgical Robotics*. Boston, MA: Springer US, 2011, pp. 159–197. [Online]. Available: http://link.springer.com/10.1007/978-1-4419-1126-1_8

[19] P. Garcia, J. Rosen, C. Kapoor, M. Noakes, G. Elbert, M. Treat, T. Ganous, M. Hanson, J. Manak, C. Hasser, D. Rohler, and R. Satava, "Trauma Pod: a semi-automated telerobotic surgical system," *The International Journal of Medical Robotics and Computer Assisted Surgery*, vol. 5, no. 2, pp. 136–146, jun 2009. [Online]. Available: http://doi.wiley.com/10.1002/rcs.238

[20] C. Freschi, V. Ferrari, F. Melfi, M. Ferrari, F. Mosca, and A. Cuschieri, "Technical review of the da Vinci surgical telemanipulator," *The International Journal of Medical Robotics and Computer Assisted Surgery*, vol. 9, no. 4, pp. 396–406, dec 2013. [Online]. Available: http://doi.wiley.com/10.1002/rcs.1468

[21] D. E.-P. Limmer, "Chapter 5 Lifting and Moving Patients," 2009.

[22] A. Williams, W. Saab, and P. Ben-Tzvi, "Analysis of Differential Mechanisms for a Robotic Head Stabilization System," in *ASME 2017 International Design Engineering Technical Conferences and Computers and Information in Engineering Conference*. ASME, aug 2017. [Online]. Available: http://proceedings.asmedigitalcollection.asme.org/proceeding.aspx?doi=10.1115/DETC2017-67371

[23] B. Sebastian, A. Williams, and P. Ben-Tzvi, "Control of a Head Stabilization System for Use in Robotic Disaster Response," in *ASME 2017 International Mechanical Engineering Congress and Exposition Volume 4A: Dynamics, Vibration, and Control*. ASME, nov 2017. [Online]. Available: http://proceedings.asmedigitalcollection.asme.org/proceeding.aspx?doi=10.1115/IMECE2017-71469

[24] A. Williams, B. Sebastian, and P. Ben-Tzvi, "A Robotic Head Stabilization Device for Medical Transport," *Journal of Mechanisms and Robotics*, vol. Submitted, March, 2018.

[25] D. J. Samuels, H. Bock, K. Mauli, and W. Stoy, *Emergency Medical Technician-Basic: National Standard Curriculum*. United States Department of Transportation National Highway Traffic Safety Administration EMT-Basic:, 1992.

[26] S. Abram and C. Bulstrode, "Routine spinal immobilization in trauma patients: What are the advantages and disadvantages?" *Surgeon*, vol. 8, no. 4, pp. 218–222, 2010. [Online]. Available: http://dx.doi.org/10.1016/j.surge.2010.01.002

[27] Department of Homeland Security, "First Responder Guide for Improving Survivability in Improvised Explosive Device and/or Active Shooter Incidents," no. June, 2015.

[28] International Federation of Red Cross and Red Crescent Societies, "World Disasters Report," Cambridge, Tech. Rep., 2015. [Online]. Available: http://reliefweb.int/sites/reliefweb.int/files/resources/1293600-World-Disasters-Report-2015_en.pdfhttp://ebooks.cambridge.org/ref/id/CBO9781107415324A009

[29] C. D. Newgard, R. H. Schmicker, J. R. Hedges, J. P. Trickett, D. P. Davis, E. M. Bulger, T. P. Aufderheide, J. P. Minei, J. S. Hata, K. D. Gubler, T. B. Brown, J. D. Yelle, B. Bardarson, and G. Nichol, "Emergency Medical Services Intervals and Survival in Trauma: Assessment of the "Golden Hour" in a North American Prospective Cohort," *Annals of Emergency Medicine*, vol. 55, no. 3, pp. 235–246.e4, 2010. [Online]. Available: http://dx.doi.org/10.1016/j.annemergmed.2009.07.024

[30] E. B. Lerner and R. M. Moscati, "The golden hour: scientific fact or medical "urban legend"?" *Academic Emergency Medicine*, vol. 8, no. 7, pp. 758–760, 2001. [Online]. Available: http://www.ncbi.nlm.nih.gov/pubmed/11435197

[31] A. M. K. Harmsen, G. F. Giannakopoulos, P. R. Moerbeek, E. P. Jansma, H. J. Bonjer, and F. W. Bloemers, "The influence of prehospital time on trauma patients outcome: A systematic review," *Injury*, vol. 46, no. 4, pp. 602–609, 2015. [Online]. Available: http://dx.doi.org/10.1016/j.injury.2015.01.008

[32] M. M. Dinh, K. Bein, S. Roncal, C. M. Byrne, J. Petchell, and J. Brennan, "Redefining the golden hour for severe head injury in an urban setting: The effect of prehospital arrival times on patient outcomes," *Injury*, vol. 44, no. 5, pp. 606–610, 2013. [Online]. Available: http://dx.doi.org/10.1016/j.injury.2012.01.011

[33] R. S. Kotwal, J. T. Howard, J. a. Orman, B. W. Tarpey, J. a. Bailey, H. R. Champion, R. L. Mabry, J. B. Holcomb, and K. R. Gross, "The Effect of a Golden Hour Policy on the Morbidity and Mortality of Combat Casualties," *JAMA Surgery*, vol. 151, no. 1, pp. 15–24, 2016. [Online]. Available: http://www.ncbi.nlm.nih.gov/pubmed/26422778

[34] B. J. Eastridge, M. Hardin, J. Cantrell, L. Oetjen-Gerdes, T. Zubko, C. Mallak, C. E. Wade, J. Simmons, J. Mace, R. Mabry, R. Bolenbaucher, and L. H. Blackbourne, "Died of wounds on the battlefield: causation and implications for improving combat casualty care." *The Journal of trauma*, vol. 71, no. 1 Suppl, pp. S4–S8, 2011.

[35] U.S. Army Medical Research and Material Command, "Unmanned Systems Teaming for Semi-Autonomous Casualty Extraction," 2017. [Online]. Available: https://sbir.defensebusiness.org/topics?topicId=28835&AspxAutoDetectCookieSupport=1

[36] P. L. Chapman, L. D. Cabrera, C. Varela-Mayer, M. M. Baker, C. Elnitsky, C. Figley, R. M. Thurman, C.-D. Lin, and L. P. Mayer, "Training, Deployment Preparation, and Combat Experiences of Deployed Health Care Personnel: Key Findings From Deployed U.S. Army Combat Medics Assigned to Line Units," *Military Medicine*, vol.

177, no. 3, pp. 270–277, mar 2012. [Online]. Available: http://www.ncbi.nlm.nih.gov/pubmed/22479913http://publications.amsus.org/doi/10.7205/MILMED-D-11-00305

[37] R. G. Snyder, "Robots assist in search and rescue efforts at WTC," *IEEE Robotics & Automation Magazine*, vol. 8, no. 4, pp. 26–28, 2001. [Online]. Available: http://cedb.asce.org/cgi/WWWdisplay.cgi?9703093

[38] R. Watts, P. Rowe, and G. Gilbert, "TATRC and TARDEC Collaborative Robots Program," APPLIED PERCEPTION INC, Tech. Rep., 2004. [Online]. Available: http://www.scopus.com/inward/record.url?eid=2-s2.0-21644476902&partnerID=tZOtx3y1

[39] Vecna Robotics, "The Bear," 2009. [Online]. Available: http://vecna.com/robotics/multimedia/downloads/BEAR.pdf

[40] G. Gilbert, T. Turner, and R. Marchessault, "Army medical robotics research," Army Telemedicine and Advanced Technology Research Center, Tech. Rep., 2007. [Online]. Available: http://oai.dtic.mil/oai/oai?verb=getRecord&metadataPrefix=html&identifier=ADA521095

[41] J. Marescaux and F. Rubino, "The ZEUS robotic system: experimental and clinical applications," *Surgical Clinics of North America*, vol. 83, no. 6, pp. 1305–1315, dec 2003. [Online]. Available: http://linkinghub.elsevier.com/retrieve/pii/S0039610903001695

[42] R. Murphy, J. Casper, J. Hyams, M. Micire, and B. Minten, "Mobility and sensing demands in USAR," *IECON Proceedings (Industrial Electronics Conference)*, vol. 1, pp. 138–142, 2000.

[43] R. R. Murphy, "A decade of rescue robots," *IEEE International Conference on Intelligent Robots and Systems*, pp. 5448–5449, 2012.

[44] K. Nagatani, S. Kiribayashi, Y. Okada, S. Tadokoro, T. Nishimura, T. Yoshida, E. Koyanagi, and Y. Hada, "Redesign of rescue mobile robot Quince," in *2011 IEEE International Symposium on Safety, Security, and Rescue Robotics*. IEEE, nov 2011, pp. 13–18. [Online]. Available: http://ieeexplore.ieee.org/xpls/abs_all.jsp?arnumber=6106794http://ieeexplore.ieee.org/document/6106794/

[45] K. Nagatani, S. Kiribayashi, Y. Okada, K. Otake, K. Yoshida, S. Tadokoro, T. Nishimura, T. Yoshida, E. Koyanagi, M. Fukushima, and S. Kawatsuma, "Emergency response to the nuclear accident at the Fukushima Daiichi Nuclear Power Plants using mobile rescue robots," *Journal of Field Robotics*, vol. 30, no. 1, pp. 44–63, jan 2013. [Online]. Available: http://doi.wiley.com/10.1002/rob.21439

[46] A. Wolf, H. Brown, R. Casciola, A. Costa, M. Schwerin, E. Shamas, and H. Choset, "A mobile hyper redundant mechanism for search and rescue tasks," in *Proceedings 2003 IEEE/RSJ International Conference on Intelligent Robots and Systems (IROS 2003) (Cat. No.03CH37453)*, vol. 3, no. October. IEEE, 2003,

pp. 2889–2895. [Online]. Available: http://ieeexplore.ieee.org/lpdocs/epic03/wrapper.htm?arnumber=1249309http://ieeexplore.ieee.org/document/1249309/

[47] A. Wolf, H. H. Choset, B. H. Brown, and R. W. Casciola, "Design and control of a mobile hyper-redundant urban search and rescue robot," *Advanced Robotics*, vol. 19, no. 3, pp. 221–248, jan 2005. [Online]. Available: http://dx.doi.org/10.1163/1568553053583652http://www.tandfonline.com/doi/abs/10.1163/1568553053583652

[48] P. Ben-Tzvi and W. Rone, "Microdroplet generation in gaseous and liquid environments," pp. 333–356, 2010.

[49] P. Ben-Tzvi, A. A. Goldenberg, and J. W. Zu, "Design and Analysis of a Hybrid Mobile Robot Mechanism With Compounded Locomotion and Manipulation Capability," *Journal of Mechanical Design*, vol. 130, no. 7, p. 072302, 2008. [Online]. Available: http://mechanicaldesign.asmedigitalcollection.asme.org/article.aspx?articleid=1449791

[50] ——, "Articulated hybrid mobile robot mechanism with compounded mobility and manipulation and on-board wireless sensor/actuator control interfaces," *Mechatronics*, vol. 20, no. 6, pp. 627–639, sep 2010. [Online]. Available: http://dx.doi.org/10.1016/j.mechatronics.2010.06.004http://linkinghub.elsevier.com/retrieve/pii/S0957415810001066

[51] G. De Cubber, "Project Public Report-ICARUS," Tech. Rep., 2012.

[52] G. De Cubber, D. Doroftei, D. Serrano, K. Chintamani, R. Sabino, and S. Ourevitch, "The EU-ICARUS project: Developing assistive robotic tools for search and rescue

operations," *2013 IEEE International Symposium on Safety, Security, and Rescue Robotics, SSRR 2013*, 2013.

[53] R. R. Murphy, *Disaster Robotics*, vol.1 ed. Cambridge: The MIT Press, 2014.

[54] B. M. Yamauchi, "PackBot: a versatile platform for military robotics," *Defense and Security*, vol. 5422, pp. 228–237, 2004. [Online]. Available: http://proceedings.spiedigitallibrary.org/proceeding.aspx?articleid=844149

[55] D. Theobald, "Mobile Extraction-Assist Robot," US Patent 7,719,222 B2, 2010.

[56] T. Atwood and J. Klein, "VECNA's Battlefild Extraction-Assist Robot BEAR," pp. 1–, 2007. [Online]. Available: https://web.archive.org/web/20101120084734/http://www.botmag.com/articles/04-25-07_vecna_bear.shtml

[57] M. Raibert, "Legged Robots," *Communications of the ACM*, vol. 29, no. 6, pp. 499–514, 1986. [Online]. Available: http://doi.acm.org/10.1145/5948.5950

[58] J. Hu and Y.-J. Lim, "Robotic First Responder System and Method," US Patent 20 140 150 806 A1, 2014.

[59] J. Ding, Y.-J. Lim, M. Solano, K. Shadle, C. Park, C. Lin, and J. Hu, "Giving patients a lift - the robotic nursing assistant (RoNA)," in *2014 IEEE International Conference on Technologies for Practical Robot Applications (TePRA)*. IEEE, apr 2014, pp. 1–5. [Online]. Available: http://ieeexplore.ieee.org/document/6869137/

[60] J. Hu, A. Edsinger, Yi-Je Lim, N. Donaldson, M. Solano, A. Solochek, and R. Marchessault, "An advanced medical robotic system augmenting healthcare capabilities - robotic nursing assistant," in *2011 IEEE International Conference on Robotics and Automation*. IEEE, may 2011, pp. 6264–6269. [Online]. Available: http://ieeexplore.ieee.org/document/5980213/

[61] J. Hu and Y.-J. Lim, "Mobile Medical Robotic System," 2012.

[62] Y. Iwano, K. Osuka, and H. Amano, "Development of stretcher component robots for rescue activity," *IEEE Conference on Robotics, Automation and Mechatronics, 2004.*, vol. 2, pp. 1–3, 2004.

[63] ——, "Development of rescue support stretcher system with stair-climbing," in *2011 IEEE International Symposium on Safety, Security, and Rescue Robotics*. IEEE, nov 2011, pp. 245–250. [Online]. Available: http://ieeexplore.ieee.org/document/6106797/

[64] N. Fisher and G. R. Gilbert, "Unmanned Systems in Support of Future Medical Operations in Dense Urban Environments," *Small Wars Journal*, 2016.

[65] K. Thompson, "Squad Multipurpose Equipment Transport (SMET)," 2015. [Online]. Available: http://www.dtic.mil/ndia/2016/GRCCE/Thompson.pdf

[66] K. Massey, "One System... Many Missions," 2016. [Online]. Available: http://www.hdtglobal.com/wp-content/uploads/2015/02/Protector_White_Paper_05.pdf

[67] ——, "Squad Mission Equipment Transport (SMET): Lessons Learned for Industry," 2016. [Online]. Available: www.dtic.mil/ndia/2016/GRCCE/Massey.pdf

[68] K. Johnson, F. Pearce, D. Westenskow, L. L. Ogden, S. Farnsworth, S. Peterson, J. White, and T. Slade, "Clinical evaluation of the Life Support for Trauma and Transport," *Critical Care*, vol. 6, no. 5, p. 439, 2002. [Online]. Available: http://ccforum.biomedcentral.com/articles/10.1186/cc1538

[69] G. C. Velmahos, D. Demetriades, M. Ghilardi, P. Rhee, P. Petrone, and L. S. Chan, "Life support for trauma and transport: A mobile ICU for safe in-hospital transport of critically injured patients," *Journal of the American College of Surgeons*, vol. 199, no. 1, pp. 62–68, 2004.

[70] M. E. Hanson, "Life Support for Trauma and Transport (LSTAT) Patient Care Platform: Expanding Global Applications and Impact," in *RTO HFM Symposium on "Combat Casualty Care in Ground Based Tactical Situations: Trauma Technology and Emergency Medical Providers"*. Integrated Medical Systems, Inc., 2004.

[71] J. Chu, "A Robomedic for the Battlefield," *MIT Technology Review*, 2009. [Online]. Available: https://www.technologyreview.com/s/411865/a-robomedic-for-the-battlefield/

[72] R. a. Beasley, "Medical Robots: Current Systems and Research Directions," *Journal of Robotics*, vol. 2012, pp. 1–14, 2012. [Online]. Available: http://www.hindawi.com/journals/jr/2012/401613/

[73] R. U. Pande, Y. Patel, C. J. Powers, G. D'ancona, and H. L. Karamanoukian, "The telecommunication revolution in the medical field: Present applications and future perspective," *Current Surgery*, vol. 60, no. 6, pp. 636–640, 2003.

[74] J. Anderson, J. Baltes, and K.-Y. Tu, "Improving Robotics Competitions for Real-World Evaluation of AI," *Proceedings of the AAAI Spring Symposium on Experimental Design for Real-World Systems*, no. January, 2009.

[75] S. Behnke, "Robot competitions-ideal benchmarks for robotics research," *Proceedings of IROS-2006 Workshop on Benchmarks in Robotics Research*, no. January 2006, 2006.

[76] A. del Pobil, "Benchmarks in robotics research," *IROS 2006 workshop*, 2006.

[77] R. Sheh, S. Schwertfeger, and A. Visser, "16 Years of RoboCup Rescue," *KI - Künstliche Intelligenz*, vol. 30, no. 3-4, pp. 267–277, oct 2016. [Online]. Available: http://link.springer.com/10.1007/s13218-016-0444-x

[78] H. Kitano, "RoboCup Rescue: a grand challenge for multi-agent systems," in *Proceedings Fourth International Conference on MultiAgent Systems*, vol. 22, no. 1. IEEE Comput. Soc, 2000, pp. 5–12. [Online]. Available: http://ieeexplore.ieee.org/document/858425/

[79] S. Tadokoro, H. Kitano, T. Takahashi, I. Noda, H. Matsubara, A. Shinjoh, T. Koto, I. Takeuchi, H. Takahashi, F. Matsuno, M. Hatayama, J. Nobe, and S. Shimada, "The RoboCup-Rescue project: a robotic approach to the

disaster mitigation problem," in *Proceedings 2000 ICRA. Millennium Conference. IEEE International Conference on Robotics and Automation. Symposia Proceedings (Cat. No.00CH37065)*, vol. 4. IEEE, 2000, pp. 4089–4094. [Online]. Available: http://ieeexplore.ieee.org/document/845369/

[80] A. Jacoff, E. Messina, and J. Evans, "A Standard Test Course for Urban Search and Rescue Robots," *Performance Metrics for Intelligent Systems Workshop*, pp. 253–259, 2000.

[81] C. D. Kidd, "Robots in Italy," *Interactions*, vol. 12, no. 2, p. 80, 2005. [Online]. Available: http://portal.acm.org/citation.cfm?doid=1052438.1052486

[82] R. Sheh and H. Komsuoglu, "The 2012 IEEE Robotics & Automation Society Safety, Security, and Rescue Robotics Summer School: An Event for the Dissemination of the Challenges and Best-in-Class Capabilities in the SSRR Community [Society News]," *IEEE Robotics & Automation Magazine*, vol. 19, no. 4, pp. 92–95, dec 2012. [Online]. Available: http://ieeexplore.ieee.org/document/6377439/

[83] G. C. Haynes, D. Stager, A. Stentz, J. M. Vande Weghe, B. Zajac, H. Herman, A. Kelly, E. Meyhofer, D. Anderson, D. Bennington, J. Brindza, D. Butterworth, C. Dellin, M. George, J. Gonzalez-Mora, M. Jones, P. Kini, M. Laverne, N. Letwin, E. Perko, C. Pinkston, D. Rice, J. Scheifflee, K. Strabala, M. Waldbaum, and R. Warner, "Developing a Robust Disaster Response Robot: CHIMP and the Robotics Challenge," *Journal of Field Robotics*, vol. 34, no. 2, pp. 281–304, 2017.

[84] S. Kim, M. M. Kim, J. Lee, S. Hwang, J. Chae, B. Park, H. Cho, J. Sim, J. Jung, H. Lee, S. Shin, M. M. Kim, N. Kwak, Y. Lee, S. Lee, M. Lee, S. Yi, K. S. K. C. Chang, and J. Park, "Approach of Team SNU to the DARPA Robotics Challenge finals," *IEEE-RAS International Conference on Humanoid Robots*, vol. 2015-Decem, pp. 777–784, 2015.

[85] S. Kohlbrecher, A. Romay, A. Stumpf, A. Gupta, O. von Stryk, F. Bacim, D. A. Bowman, A. Goins, R. Balasubramanian, and D. C. Conner, "Human-robot Teaming for Rescue Missions: Team ViGIR's Approach to the 2013 DARPA Robotics Challenge Trials," *Journal of Field Robotics*, vol. 32, no. 3, pp. 352–377, may 2015.

[86] A. Matos, A. Martins, A. Dias, B. Ferreira, J. M. Almeida, H. Ferreira, G. Amaral, A. Figueiredo, R. Almeida, and F. Silva, "Multiple robot operations for maritime search and rescue in euRathlon 2015 competition," in *OCEANS 2016 - Shanghai*. IEEE, apr 2016, pp. 1–7. [Online]. Available: http://ieeexplore.ieee.org/document/7485707/

[87] A. F. T. Winfield, B. Brueggemann, A. Castro, and M. Cordero, "euRathlon 2015: a multi-domain multi-robot Grand Challenge for Search and Rescue Robots," no. September 2014, 2015.

[88] F. E. Schneider, D. Wildermuth, and I. Processing, "European Land Robot Trial (ELROB) Towards a Realistic Benchmark for Outdoor Robotics," *Proceedings of the 1st iIternational Conference on Robotics in Education*, pp. 65–70, 2007.

[89] P. Corke, *Field and Service Robotics*, ser. Springer Tracts in Advanced Robotics, D. S. Wettergreen and T. D. Barfoot, Eds. Cham: Springer International Publishing, 2016, vol. 113.

[90] T. Simonite, "Automated Anesthesiologist Suffers a Painful Defeat," *MIT Technology Review*, 2016. [Online]. Available: https://www.technologyreview.com/s/601141/automated-anesthesiologist-suffers-a-painful-defeat/

[91] P. Ben-Tzvi, A. Williams, B. Sebastian, A. Kumar, and W. Saab, "Semi-Autonomous Victim Extraction Robot (SAVER)," US Provisional Patent Application No. 62/660,869, April 20, 2018.

[92] M. Bernhard, A. Gries, P. Kremer, and B. W. Bottiger, "Spinal cord injury (SCI) - Prehospital management," *Resuscitation*, vol. 66, no. 2, pp. 127–139, 2005.

[93] M. N. Hadley, B. C. Walters, P. A. Grabb, N. M. Oyesiku, G. J. Przybylski, D. K. Resnick, T. C. Ryken, and D. H. Mielke, "Guidelines for the management of acute cervical spine and spinal cord injuries." *Clinical Neurosurgery*, vol. 49, pp. 407–98, 2002. [Online]. Available: http://www.ncbi.nlm.nih.gov/pubmed/12506565

[94] R. A. Connell, C. A. Graham, and P. T. Munro, "Is spinal immobilisation necessary for all patients sustaining isolated penetrating trauma?" *Injury*, vol. 34, no. 12, pp. 912–914, 2003.

[95] T. Sundstrøm, H. Asbjørnsen, S. Habiba, G. A. Sunde, and K. Wester, "Prehospital use of cervical collars in trauma patients: a critical review." *Journal of neurotrauma*,

vol. 31, no. 6, pp. 531–40, 2014. [Online]. Available: http://www.pubmedcentral.nih.gov/articlerender.fcgi?artid=3949434&tool=pmcentrez&rendertype=abstract

[96] M. N. Hadley, B. C. Walters, B. Aarabi, S. Dhall, D. Gelb, M. Harrigan, R. J. Hurlbert, C. Rozzelle, T. Ryken, and N. Theodore, "Updated Guidelines for the Management of Acute Cervical Spine and Spinal Cord Injury." *Neurosurgery*, vol. 72 Suppl 2, no. 3, mar 2013. [Online]. Available: http://www.tandfonline.com/doi/abs/10.1080/17450918.2010.497851http://content.wkhealth.com/linkback/openurl?sid=WKPTLP:landingpage&an=00006123-201303002-00001http://www.ncbi.nlm.nih.gov/pubmed/23417171

[97] M. Kreinest, B. Gliwitzky, S. Schüler, P. A. Grützner, and M. Münzberg, "Development of a New Emergency Medicine Spinal Immobilization Protocol for Trauma Patients and a Test of Applicability by German Emergency Care Providers," *Scandinavian Journal of Trauma, Resuscitation and Emergency Medicine*, vol. 24, no. 1, 2016. [Online]. Available: http://sjtrem.biomedcentral.com/articles/10.1186/s13049-016-0267-7

[98] C. Vaillancourt, I. G. Stiell, T. Beaudoin, J. Maloney, A. R. Anton, P. Bradford, E. Cain, A. Travers, M. Stempien, M. Lees, D. Munkley, E. Battram, J. Banek, and G. A. Wells, "The Out-of-Hospital Validation of the Canadian C-Spine Rule by Paramedics," *Annals of Emergency Medicine*, vol. 54, no. 5, pp. 663–671, 2009. [Online]. Available: http://dx.doi.org/10.1016/j.annemergmed.2009.03.008

[99] M. Hauswald, G. Ong, D. Tandberg, and Z. Omar, "Out-of-hospital spinal immobilization: its effect on neurologic injury." *Academic emergency medicine : official journal of the Society for Academic Emergency Medicine*, vol. 5, no. 3, pp. 214–219, 1998.

[100] M. Holla, J. M. R. Huisman, N. Verdonschot, J. Goosen, A. J. F. Hosman, and G. Hannink, "The ability of external immobilizers to restrict movement of the cervical spine: a systematic review," *European Spine Journal*, vol. 25, no. 7, pp. 2023–2036, 2016.

[101] L. E. Stuke, P. T. Pons, J. S. Guy, W. P. Chapleau, F. K. Butler, and N. E. McSwain, "Prehospital spine immobilization for penetrating trauma-review and recommendations from the prehospital trauma life support executive committee." *The Journal of trauma*, vol. 71, no. 3, pp. 763–770, 2011.

[102] D. Jaslow M.D, "Best Practices : Myths and Realities of Spinal Immobilization," 2006. [Online]. Available: http://www.emsworld.com/article/10322876/best-practices-myths-and-realities-of-spinal-immobilization

[103] L. Birglen and C. Gosselin, "Force Analysis of Connected Differential Mechanisms: Application to Grasping," *The International Journal of Robotics Research*, vol. 25, no. 10, pp. 1033–1046, oct 2006. [Online]. Available: http://ijr.sagepub.com/cgi/doi/10.1177/0278364906068942

[104] M. Yim and J. Laucharoen, "Towards small robot aided victim manipulation," *Journal of Intelligent and Robotic Systems: Theory and Applications*, vol. 64, no. 1, pp. 119–139, 2011.

[105] M. Gallagher, K. Li, A. Terraciano, B. Banisadr, M. Maltese, and A. Jackson, "MechaNek." [Online]. Available: http://www.mechanek.com/

[106] S. Hirose, "Connected Differential Mechanism and its Applications," in *Proceedings of 1985 Int. Conf. on Advanced Robotics*, 1985, pp. 319–325.

[107] M. Baril, T. Laliberté, C. Gosselin, and F. Routhier, "On the Design of a Mechanically Programmable Underactuated Anthropomorphic Prosthetic Gripper," *Journal of Mechanical Design*, vol. 135, no. 12, pp. 121 008 1–12, 2013. [Online]. Available: http://dx.doi.org/10.1115/1.4025493%5Cnhttp://mechanicaldesign.asmedigitalcollection.asme.org/data/Journals/JMDEDB/927630/md_135_12_121008.pdf

[108] J. T. Belter and A. M. Dollar, "Novel differential mechanism enabling two DOF from a single actuator: Application to a prosthetic hand," in *2013 IEEE 13th Int. Conf. on Rehabilitation Robotics (ICORR)*. IEEE, jun 2013, pp. 1–6. [Online]. Available: http://ieeexplore.ieee.org/document/6650441/

[109] G. P. Kontoudis, M. V. Liarokapis, A. G. Zisimatos, C. I. Mavrogiannis, and K. J. Kyriakopoulos, "Open-source, anthropomorphic, underactuated robot hands with a selectively lockable differential mechanism: Towards affordable prostheses," *IEEE International Conference on Intelligent Robots and Systems*, vol. 2015-Decem, pp. 5857–5862, 2015.

[110] R. M. Crowder, "An anthropomorphic robotic end effector," *Robotics and Autonomous Systems*, vol. 7, no. 4, pp. 253–268, 1991.

[111] Y. Kamikawa and T. Maeno, "Underactuated five-finger prosthetic hand inspired by grasping force distribution of humans," in *2008 IEEE/RSJ Int. Conf. on Intelligent Robots and Systems*. IEEE, sep 2008, pp. 717–722. [Online]. Available: http://ieeexplore.ieee.org/document/4650628/

[112] M. Rakić, "Multifingered robot hand with selfadaptability," *Robotics and Computer Integrated Manufacturing*, vol. 5, no. 2-3, pp. 269–276, 1989.

[113] T. Laliberté and C. Gosselin, "Actuation System for Highly Underactuated Gripping System," 2003.

[114] L. Birglen, T. Laliberté, and C. Gosselin, "Underactuated Robotic Hands," in *Springer Tracts in Advanced Robotics*, 2008, pp. 33–60. [Online]. Available: http://www.scopus.com/inward/record.url?eid=2-s2.0-37549012181&partnerID=tZOtx3y1

[115] C. Y. Brown and H. H. Asada, "Inter-finger coordination and postural synergies in robot hands via mechanical implementation of principal components analysis," *IEEE International Conference on Intelligent Robots and Systems*, pp. 2877–2882, 2007.

[116] M. Baril, T. Laliberté, F. Guay, and C. Gosselin, "Static analysis of single-input/multiple-output tendon-driven underactuated mechanisms for robotic hands," in *ASME 2010 Int. Design Engineering Technical Conf. and Computers and Information in Engineering Conf., IDETC/CIE2010*, vol. 2, 2010, pp. 155–164. [Online]. Available: https://www.scopus.com/inward/record.uri?eid=2-s2.0-80055006047&partnerID=40&md5=e099fb1e23ffc5222b781c6486005054

[117] H. Khakpour, L. Birglen, and S. A. Tahan, "Synthesis of differentially driven planar cable parallel manipulators," *IEEE Transactions on Robotics*, vol. 30, no. 3, pp. 619–630, 2014.

[118] F. Almeida, A. Lopes, and P. Abreu, "Force-Impedance Control : a new control strategy of robotic manipulators," *Advanced intelligent mechatronics*, pp. 1–12, 1999.

[119] I. Jo and J. Bae, "Design and control of a wearable and force-controllable hand exoskeleton system," *Mechatronics*, vol. 41, no. c, pp. 90–101, 2017.

[120] R. C. Luo, C. C. Chang, and Y. W. Perng, "Impedance control on a multi-fingered robot hand based on analyzed electromyographic information for massage applications," *IEEE International Symposium on Industrial Electronics*, no. ISlE, pp. 1228–1233, 2009.

[121] D. W. Robinson, J. E. Pratt, D. J. Paluska, and G. A. Pratt, "Series Elastic Actuator Development for a Biomimetic Walking Robot," *Proceedings of the 1999 IEEE/ASME International Conference on Advanced Intelligent Machines*, pp. 561–568, 1999.

[122] G. A. Pratt and M. M. Williamson, "Series elastic actuators," *IEEE/RSJ International Conference on Intelligent Robots and Systems. 'Human Robot Interaction and Cooperative Robots'*, vol. 1, no. 1524, pp. 399–406, 1995. [Online]. Available: http://ieeexplore.ieee.org/lpdocs/epic03/wrapper.htm?arnumber=525827

[123] P. Bernhardt, H. J. Wilke, K. H. Wenger, B. Jungkunz, A. Böhm, and L. E. Claes, "Multiple muscle force simulation in axial rotation of the cervical spine," *Clinical Biomechanics*, vol. 14, no. 1, pp. 32–40, 1999.

[124] Actuonix Motion Devices Inc., "Actuonix L16 Datasheet," pp. 1–3.

[125] J. Han, "From PID to Active Disturbance Rejection Control," *IEEE Transactions on Industrial Electronics*, vol. 56, no. 3, pp. 900–906, mar 2009. [Online]. Available: http://ieeexplore.ieee.org/document/4796887/

[126] Zhiqiang Gao, "Scaling and bandwidth-parameterization based controller tuning," in *Proceedings of the 2003 American Control Conference, 2003.*, vol. 6. IEEE, 2003, pp. 4989–4996. [Online]. Available: http://ieeexplore.ieee.org/document/1242516/

[127] G. Herbst, *A Simulative Study on Active Disturbance Rejection Control (ADRC) as a Control Tool for Practitioners*, 2013, vol. 2, no. 3. [Online]. Available: http://www.mdpi.com/2079-9292/2/3/246/

[128] R. Miklosovic, A. Radke, and Z. Gao, "Discrete implementation and generalization of the extended state observer," *2006 American Control Conference*, pp. 2209–2214, 2006.